PROBLEMS IN NONLINEAR ANALYSIS OF MOVEMENTS IN SOILS

by

NEIL EDWARD WEDGE

B.A.Sc., University of British Columbia, 1974

A THESIS SUBMITTED IN PARTIAL FULFILLMENT OF
THE REQUIREMENTS FOR THE DEGREE OF
MASTER OF APPLIED SCIENCE

in

THE FACULTY OF GRADUATE STUDIES
(Department of Civil Engineering)

We accept this thesis as conforming
to the required standard

THE UNIVERSITY OF BRITISH COLUMBIA

March, 1977

In presenting this thesis in partial fulfilment of the requirements for an advanced degree at the University of British Columbia, I agree that the Library shall make it freely available for reference and study. I further agree that permission for extensive copying of this thesis for scholarly purposes may be granted by the Head of my Department or by his representatives. It is understood that copying or publication of this thesis for financial gain shall not be allowed without my written permission.

Department of Civil Engineering

The University of British Columbia
2075 Wesbrook Place
Vancouver, Canada
V6T 1W5

Date March, 1977

ABSTRACT

The problems associated with nonlinear analysis of the load-deformation response of soils and soil structures are investigated. Methods of incremental nonlinear analysis are reviewed and their relative advantages and disadvantages discussed. Stress-strain relations commonly used for soils are critically examined and their limitations discussed. These stress-strain relations are based on the assumption that soils are isotropic, incrementally elastic materials. Evidence reported by other authors and reviewed in this study shows that the stress-strain relations commonly used for soils have two major sources of error, the anisotropy of soils and the effects of stress-path are neglected. The representation of soil stress-strain behaviour after yield is discussed. Although soils act as plastic materials after yield, it is common practice to represent post-yield behaviour by models of elastic materials. Many researchers use a constant value of Poisson's ratio and merely reduce the value of Young's modulus at yield. It is shown, with numerical examples, that this practice results in yielded soil elements being unrealistically compressible after yield. It is shown, with further numerical examples, that the predicted behaviour of yielded soil elements is more realistic if the value of the shear modulus is reduced at yield and the bulk modulus is not reduced.

TABLE OF CONTENTS

LIST OF FIGURES

NOTATION

The following is a list of the symbols used in this thesis and their definitions.

b	=	the inverse of asymptotic value of the resultant deviatoric stress
B	=	the ratio of the shear modulus after yield to that before yield
c	=	the cohesion intercept of Mohr-Coulomb failure envelope
d	=	the rate of increase of the tangent value of Poisson's ratio with strain
dV	=	an infinitesimal change in volume
E_i	=	the initial tangent value of Young's modulus
E_t	=	the tangent value of Young's modulus
F	=	the decrease in the tangent value of Poisson's ratio for a tenfold increase in the minor principal stress
G	=	the tangent value of Poisson's ratio for an isotropic stress equal to atmospheric pressure
G_i	=	the initial tangent value of the shear modulus
G_t	=	the tangent shear modulus
h	=	the depth below the soil surface
K	=	Young's modulus number
K_i	=	the initial tangent value of the bulk modulus
K_t	=	the tangent value of the bulk modulus
K_o	=	the coefficient of lateral earth pressure at rest

$\overline{K}$	=	the slope of stress-strain curve for the one-dimensional case at the end of the last load increment
m	=	the rate of change of the tangent bulk modulus with the mean normal stress
M_i	=	the initial tangent value of the constrained modulus
M_t	=	the tangent value of the constrained modulus
n	=	Young's modulus exponent
N	=	a number that indicates the rate of increase of the tangent bulk modulus with respect to a normalized volumetric strain
p_a	=	atmospheric pressure
q_i	=	the displacement at the end of the ith load increment
Q_i	=	the load at the end of the ith load increment
$q_{i,n}$	=	the nth approximation of the displacement at the end of the ith load increment
$Q_{i,\frac{1}{2}}$	=	the average load for the ith load increment
R	=	the ratio of Young's modulus before yield to that after yield
R_f	=	the failure ratio
S	=	the stress-level
S_d	=	the resultant deviatoric stress
V	=	volume
ε_d	=	the resultant deviatoric strain
ε_i	=	the strain at the end of the ith load increment
$\varepsilon_{i,n}$	=	the nth approximation of the ith load increment
ε_v	=	the volumetric strain

ε_{vc} = the characteristic volumetric strain

ε_{vn} = the normalized volumetric strain

γ = the unit weight

γ_{ij} = the shear strain for the i plane in the j direction

Δq_i = the change in displacement in the ith load increment

ΔQ_i = the ith increment of load

ζ_i = the ith natural coordinate

σ_i = the stress at the end of the ith load increment

σ_1 = the major principal stress

σ_3 = the minor principal stress

$(\sigma_1-\sigma_3)_{ult}$ = the asymptotic deviator stress

$(\sigma_1-\sigma_3)_f$ = the deviator stress at failure

σ_1' = the major principal effective stress

σ_3' = the minor principal effective stress

σ^e = the error in a calculated stress

σ_m = the mean normal stress

ν_1 = the value of Poisson's ratio before yield

ν_2 = the value of Poisson's ratio after yield

ν_t = the tangent value of Poisson's ratio

τ_{ij} = the shear stress on the i plane in the j direction

ϕ = the angle of internal friction

ϕ' = the effective angle of internal friction

Vectors:

$\{q\}_o$ = the vector of initial nodal displacements

$\{q\}_i$ = the vector of nodal displacements at the end of the ith load increment

$\{q\}_{i,n}$ = the nth approximation of the nodal displacement vector at the end of the ith load increment

$\{Q\}_o$ = the initial nodal force vector

$\{Q\}_i$ = the nodal force vector at the end of the ith load increment

$\{Q^e\}_{i,n}$ = the nth vector of nodal correction forces for the ith load increment

$\{\varepsilon\}_o$ = the vector of initial element strains

$\{\varepsilon\}_i$ = the vector of element strains at the end of the ith load increment

$\{\varepsilon\}_{i,n}$ = the nth approximation of the vector of element strains at the end of the ith load increment

$\delta\{q\}$ = a vector of virtual nodal displacements

$\delta\{\varepsilon\}$ = a vector of virtual element strains

$\{\Delta q\}_i$ = the change in the vector of nodal displacements during the ith load increment

$\{\Delta q\}_{i,n}$ = the nth approximation of the change in the vector of nodal displacements for the ith load increment

$\{\Delta q\}'_{i,n}$ = the nth correction to the vector of nodal displacements at the end of the ith load increment

$\{\Delta Q\}_i$ = the ith increment of nodal forces

$\{\Delta\varepsilon\}_i$ = the change in the vector of element strains for the ith load increment

$\{\Delta\varepsilon\}_{i,n}$ = the nth approximation of the change in the vector of element strains for the ith load increment

$\{\Delta\varepsilon\}'_{i,n}$ = the nth correction to the vector of element strains at the end of the ith load increment

$\{\Delta\sigma\}_i$ = the change in the vector of element stresses for the ith load increment

$\{\Delta\sigma\}_{i,n}$ = the nth approximation of the change in the vector of nodal displacements for the ith load increment

$\{\sigma\}_o$ = the vector of initial element stresses

$\{\sigma\}_i$ = the vector of element stresses at the end of the ith load increment

$\{\sigma\}_{i,\frac{1}{2}}$ = the vector of average element stresses for the ith load increment

$\{\sigma\}_{i,j-\frac{1}{2}}$ = the jth approximation of the vector of average element stresses for the ith load increment

$\{\sigma^e\}_i$ = the vector of errors in element stresses for the end of the ith load increment

$[B]_e$ = the element strain-displacement matrix

$[D]$ = the stress-strain matrix

$[D]_e$ = the element stress-strain matrix

$[D]_{ei}$ = the element stress-strain matrix appropriate to the ith load increment

$[D]_{ei,n}$ = the nth approximation of the element stress-strain matrix appropriate to the ith load increment

$[K_T]$ = the global tangent stiffness matrix

$[K_T]_i$ = the global tangent stiffness matrix appropriate to the ith load increment

$[K_T]_e$ = the element tangent stiffness matrix

$[K_T]_{ei}$ = the element tangent stiffness matrix appropriate to the ith load increment

$[K_T]_{ei,n}$ = the nth approximation of the element tangent stiffness matrix appropriate to the ith load increment

ACKNOWLEDGEMENTS

The writer gratefully acknowledges the advice and guidance given by his supervisor, Dr. W.D. Liam Finn, the advice of Dr. N.D. Nathan, and the advice and generous assistance given by Dr. K. Lee. Special thanks are due to Miss Desirée Cheung for typing the manuscript.

CHAPTER 1

INTRODUCTION

The finite element method of analysis has been used extensively (5,8,9,11,12,18) to predict deformations in soil structures and movements of foundations under various kinds of applied loadings. This method provides the most convenient means of representing the geometrical, kinematical and equilibrium relations of soil structures. It also allows the use of stress-strain relations in the form of either analytical or discrete data.

The effectiveness of the method in predicting the deformations of soil structures is limited mainly by the adequacy with which the stress-strain relations and failure conditions for soils can be represented.

The modelling of soil stress-strain behaviour prior to failure is not a simple problem. The stress-strain relations of soils are nonlinear, stress dependent and stress-path dependent (9,10,13,17,18).

The failure criteria for soils are not firmly established and the post-failure behaviour is open to a variety of interpretations.

Once a model for the stress-strain behaviour of soil has been adopted, one of two general methods of nonlinear analysis may be used to predict the deformations of

soil structures under applied loadings. One method, known as iterative elastic analysis, consists of applying the entire loading in one step and iterating on the stress-strain properties used in order to obtain strains which are compatible with the applied loads and the stress-strain model of the soil. In the second method, which is called incremental analysis, the loading is applied in suitable increments and the stress-strain behaviour of the soil is assumed to be linear within each load increment. In the analysis of each load increment one may iterate on the stress-strain properties used in order to obtain strains which at the end of the increment, are compatible with the applied loads and the stress-strain model of the soil.

The incremental technique has the advantage that it allows the determination of the load-displacement history of the soil body up to the loading of interest, rather than just the deformations corresponding to the final loading as in the case of iterative elastic analysis.

The purpose of this study is to investigate the problems associated with the use of existing stress-strain relations in the incremental nonlinear analysis of soil deformations.

CHAPTER 2

METHODS OF INCREMENTAL ANALYSIS FOR NONLINEAR MATERIALS

2.1 General Discussion of Incremental Analysis

A nonlinear material is one for which the relationship between the applied stresses and the resulting strains is nonlinear.

The tangent moduli for such a material are the instantaneous slopes of the stress-strain curves and they may be expressed in terms of the stresses or strains at the point of interest. For example,

$$E_t = E_t(\{\sigma\}) \text{ or } E_t(\{\varepsilon\}) \tag{2-1}$$

and

$$\nu_t = \nu_t(\{\sigma\}) \text{ or } \nu_t(\{\varepsilon\}) \tag{2-2}$$

where E_t is the tangent value of Young's modulus, ν_t is the tangent value of Poisson's ratio, $\{\sigma\}$ is the state of stress, and $\{\varepsilon\}$ is the state of strain.

Since the stiffness matrix of a finite element depends upon the values of the moduli, it is also a function of the state of stress or strain existing in that element. Hence, the tangent stiffness matrix of the element based upon the tangent moduli is $[K_T]_e$,

$$[K_T]_e = [K_T(\{\sigma\})]_e \text{ or } [K_T(\{\varepsilon\})]_e \tag{2-3}$$

The states of stress and strain change during the loading of the finite element and, as a result, no single value of the tangent stiffness matrix is applicable during the entire analysis.

One method of dealing with the stress or strain dependency of the tangent stiffness matrix is to load the structure in increments and to assume that the material behaves linearly within each load increment. This approximation to the true stress-strain response is shown in Figure 1 for the one-dimensional case.

For a body which has been divided into a number of finite elements the general approach is as follows:

The total load vector, $\{Q\}$, to be applied is divided into n load increments $\{\Delta Q\}_i$. If $\{Q\}_o$ is the initial load vector acting on the body, then the load vector, $\{Q\}_i$, acting at the end of the ith load increment is given by

$$\{Q\}_i = \{Q\}_o + \sum_{j=1}^{i} \{\Delta Q\}_j \qquad (2\text{-}4)$$

For the ith load increment, $\{\Delta Q\}_i$,

$$[K_T]\ \{\Delta q\}_i = \{\Delta Q\}_i \qquad (2\text{-}5)$$

where $[K_T]$ is the global stiffness matrix based on the tangent moduli appropriate to the element stresses in the ith load increment and $\{\Delta q\}_i$ is the incremental nodal displacement vector resulting from the application of $\{\Delta Q\}_i$.

The increments of element stress resulting from

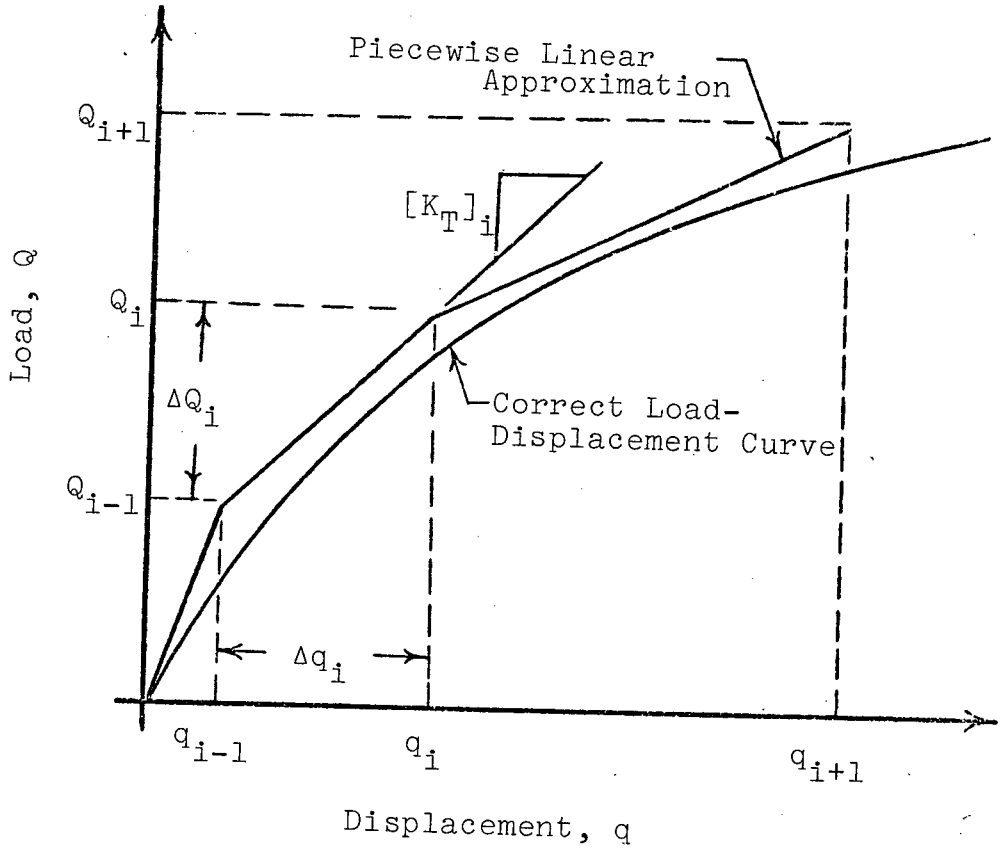

FIGURE 1 INCREMENTAL APPROXIMATION OF A NONLINEAR LOAD-DEFLECTION CURVE

the application of the ith load increment are not known when one begins the analysis of the increment. Therefore, both the moduli and the global stiffness matrix appropriate to the load increment are unknown when one begins the analysis of the increment. An iterative procedure must be used in order to find these.

The total nodal displacement vector, $\{q\}_i$, at the end of the ith load increment is given by

$$\{q\}_i = \{q\}_o + \sum_{j=1}^{i} \{\Delta q\}_j \tag{2-6}$$

where $\{q\}_o$ is the vector of initial nodal displacements.

For a particular finite element, the incremental strain vector, $\{\Delta\varepsilon\}_i$, resulting from the application of the ith load increment is given by

$$\{\Delta\varepsilon\}_i = [B]_e \{\Delta q\}_i \tag{2-7}$$

where $[B]_e$ is the strain-displacement matrix for the element which depends only upon the initial geometry of the element if geometrical nonlinearity is negligible.

The total strain vector, $\{\varepsilon\}_i$, for the element, at the end of the ith load increment is given by

$$\{\varepsilon\}_i = \{\varepsilon\}_o + \sum_{j=1}^{i} \{\Delta\varepsilon\}_j \tag{2-8}$$

where $\{\varepsilon\}_o$ is the initial strain vector.

The incremental stress vector, $\{\Delta\sigma\}_i$, for the element, for the ith load increment is given by

$$\{\Delta\sigma\}_i = [D]_e \{\Delta\varepsilon\}_i \tag{2-9}$$

where $[D]_e$ is the element stress-strain matrix appropriate to the ith load increment, which depends upon the element stresses in the increment and must be found by an iterative procedure.

The total element stress vector, $\{\sigma\}_i$, at the end of the ith load increment is given by

$$\{\sigma\}_i = \{\sigma\}_o + \sum_{j=1}^{i} \{\Delta\sigma\}_j \qquad (2\text{-}10)$$

where $\{\sigma\}_o$ is the initial element stress vector.

2.2 Iterative Methods

2.2.1 One Iteration per Load Increment

The first method to be considered is an attempt to improve the estimates of the stress-strain matrix, $[D]_{ei}$, and the stiffness matrix, $[K_T]_i$, used in the ith load increment without using a convergence criterion. The method was suggested by Duncan (8).

Each load increment is analysed twice. The first time, the tangent moduli for the finite elements are calculated from the initial stress condition for the increment. These moduli are used to calculate the element stress-strain matrices, $[D]_{ei,1}$, and the element stiffness matrices, $[K]_{ei,1}$, for the ith load increment. That is

$$[D]_{ei,1} = [D(\{\sigma\}_{i-1})]_e \qquad (2\text{-}11)$$

and

$$[K_T]_{ei,1} = [K_T(\{\sigma\}_{i-1})]_e \qquad (2\text{-}12)$$

for a particular element. The element stiffness matrices

are used to calculate the global stiffness matrix, $[K_T]_{i,1}$, which is then used to calculate the incremental nodal deflections, $\{\Delta q\}_{i,1}$, from which the incremental element strains, $\{\Delta\varepsilon\}_{i,1}$, are determined. The incremental element stresses, $\{\Delta\sigma\}_{i,1}$, are then computed using $[D]_{ei,1}$ in Equation (2-9). Since the behaviour of the material is assumed to be linear within each load increment, the average state of stress in a given element during the load increment, $\{\sigma\}_{i,\frac{1}{2}}$, is given by

$$\{\sigma\}_{i,\frac{1}{2}} = \{\sigma\}_{i-1} + \tfrac{1}{2}\{\Delta\sigma\}_{i,1} \qquad (2\text{-}13)$$

in which $\{\sigma\}_{i-1}$ is the element stress vector at the end of the preceding load increment. Improved estimates of the moduli are obtained by using the average stress state defined by Equation (2-13). The corresponding element stress-strain and stiffness matrices are then computed as

$$[D]_{ei,2} = [D(\{\sigma\}_{i,\frac{1}{2}})]_e \qquad (2\text{-}14)$$

and

$$[K_T]_{ei,2} = [K_T(\{\sigma\}_{i,\frac{1}{2}})]_e \qquad (2\text{-}15)$$

The response to the ith load increment is analysed once more using the improved estimates of the stress-strain and stiffness matrices. The process is illustrated in Figure 2.

Since no convergence criterion is used and only one iteration is performed, the factor controlling the accuracy with which the true stress-strain curve of the material is followed is the size of the load increments.

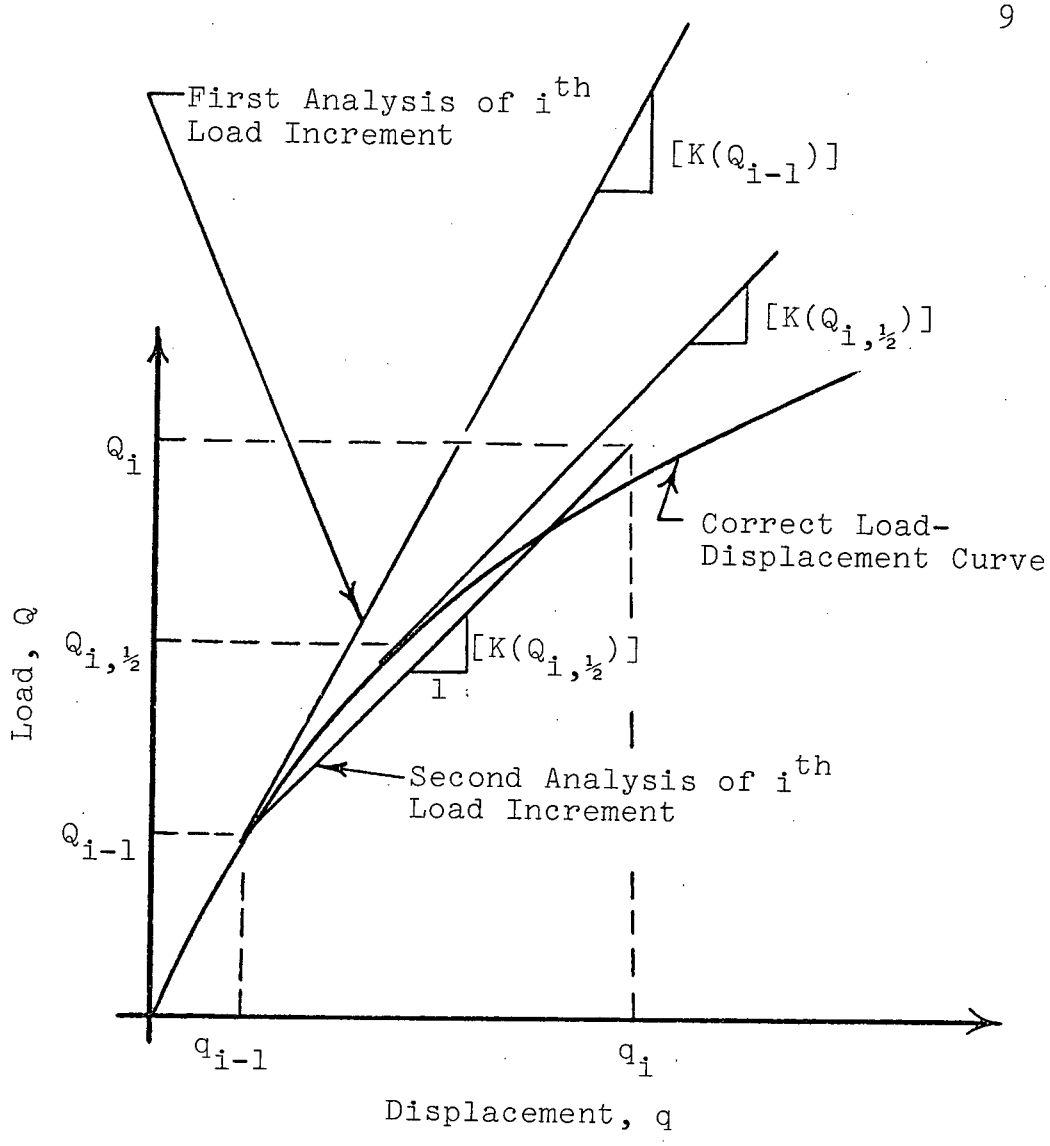

FIGURE 2 ONE ITERATION PER LOAD INCREMENT METHOD

2.2.2. Iterations Using a Convergence Criterion

The accuracy of the method described above can be increased by continuing iterations until some convergence criterion, such as a sufficiently small change in the moduli between two iterations, is satisfied.

From the jth analysis of the ith load increment

$$\{\sigma\}_{i,j-\frac{1}{2}} = \{\sigma\}_{i-1} + \tfrac{1}{2}\{\Delta\sigma\}_{i,j} \tag{2-16}$$

and for the $(j+1)^{th}$ analysis of the increment

$$[D]_{ei,j+1} = [D(\{\sigma\}_{i,j-\frac{1}{2}})]_e \tag{2-17}$$

$$[K_T]_{ei,j+1} = [K_T(\{\sigma\}_{i,j-\frac{1}{2}})]_e \tag{2-18}$$

$$\{\Delta q\}_{i,j+1} = [K_T]^{-1}_{i,j+1}\{\Delta Q\}_i \tag{2-19}$$

$$\{\Delta\varepsilon\}_{i,j+1} = [B]_e\ \{\Delta q\}_{i,j+1} \tag{2-20}$$

and

$$\{\Delta\sigma\}_{i,j+1} = [D]_{ei,j+1}\ \{\Delta\varepsilon\}_{i,j+1} \tag{2-21}$$

for $j \geq 1$.

The process is continued until the change in moduli from one iteration to the next satisfies the convergence criterion. If this occurs on the nth analysis of the load increment, then

$$\{q\}_i = \{q\}_{i-1} + \{\Delta q\}_{i,n} \tag{2-22}$$

$$\{\varepsilon\}_i = \{\varepsilon\}_{i-1} + \{\Delta\varepsilon\}_{i,n} \tag{2-23}$$

and

$$\{\sigma\}_i = \{\sigma\}_{i-1} + \{\Delta\sigma\}_{i,n} \tag{2-24}$$

2.2.3 Application of Correction Forces

In both of the methods discussed above one attempts to achieve agreement between the predicted stresses and strains at the end of the ith load increment and the true stress-strain relation of the material by adjusting the stress-strain properties used in the analysis of the increment.

An alternative method of obtaining agreement between the predicted stresses and strains and the true stress-strain relation of the material which might be used in conjunction with the methods discussed above is given here.

At the end of the ith load increment, in any incremental loading procedure, the calculated stress vector, $\{\sigma\}_i$, and calculated strain vector, $\{\varepsilon\}_i$, for a particular finite element, may not be compatible with the stress-strain relation of the material. If the stress-strain relation of the material is expressed by

$$\{\sigma\} = f(\{\varepsilon\}) \tag{2-25}$$

then, if the strains are assumed to be correct, the error in the calculated stress vector, $\{\sigma\}_i$, is given by

$$\{\sigma^e\}_i = \{\sigma\}_i - f(\{\varepsilon\}_i) \tag{2-26}$$

where $\{\sigma^e\}_i$ is the error in the calculated stress vector and $f(\{\varepsilon\}_i)$ is the true stress. This error may be balanced by applying nodal correction forces, $\{Q^e\}$, to the element at

the beginning of the $(i+1)^{th}$ load increment.

By the principle of virtual work

$$\int \delta\{\varepsilon\}^T \{\sigma^e\}_i dV = \delta\{q\}^T \{Q^e\} \tag{2-27}$$

where $\delta\{\varepsilon\}^T$ is a vector of virtual strains and $\delta\{q\}^T$ is a vector of virtual nodal displacements.

Introducing the relation $\delta\{\varepsilon\}^T = \delta\{q\}^T [B]_e^T$ in Equation (2-27) yields

$$\int \delta\{q\}^T [B]_e^T \{\sigma^e\}_i dV = \delta\{q\}^T \{Q^e\} \tag{2-28}$$

and since $\delta\{q\}^T$ is arbitrary and not a function of position

$$\{Q^e\} = \int [B]_e^T \{\sigma^e\}_i dV \tag{2-29}$$

Furthermore, if $\{\sigma^e\}_i$ is not a function of position

$$\{Q^e\} = \left[\int [B]_e^T \, dV \right] \{\sigma^e\}_i \tag{2-30}$$

2.2.4 Modified Newton-Raphson Method

In the methods described in sections (2.2.1) and (2.2.2) one attempts to make the element stresses, $\{\sigma\}_i$, and element strains, $\{\varepsilon\}_i$, at the end of the ith load increment compatible with the stress-strain relation of the material by adjusting the stress-strain properties used in the analysis of the response to the increment by rebuilding the element and global stiffness matrices and repeating the analysis of the response to the increment. The subsequent analyses of the response to the load increment yield new

estimates of the nodal displacements, $\{q\}_i$, the element strains, $\{\varepsilon\}_i$, and the element stresses, $\{\sigma\}_i$, at the end of the increment.

It is possible to make the element stresses, $\{\sigma\}_i$, and the element strains, $\{\varepsilon\}_i$, agree with the stress-strain relation of the material without adjusting the stress-strain properties used in the analysis of the response to the ith load increment.

Consider the one-dimensional case (Figure 3). The equilibrium stress $\sigma_{i,1}$, and the strain $\varepsilon_{i,1}$, obtained in the first analysis of the response to the ith load increment, do not agree with the stress-strain relation of the material. If one assumes that the equilibrium stress, $\sigma_{i,1}$, is the correct stress for the end of the ith load increment, one may obtain better agreement, while maintaining equilibrium, by adjusting the estimate of the strain using the Newton-Raphson method. If $\overline{K}$ is the slope of the stress-strain curve of the material at the beginning of the ith load increment, and $\varepsilon_{i,n}$ is the nth approximation of the correct strain corresponding to $\sigma_{i,1}$ and σ^e is defined by

$$\sigma^e = \sigma_{i,1} - f(\varepsilon_{i,n}) \tag{2-31}$$

in which $f(\varepsilon_{i,n})$ is the stress prescribed by the stress-strain relation of the material for $\varepsilon_{i,n}$, then an improved estimate, $\varepsilon_{i,n+1}$, of the correct strain is given by

$$\varepsilon_{i,n+1} = \varepsilon_{i,n} + \frac{\sigma^e}{\overline{K}} \tag{2-32}$$

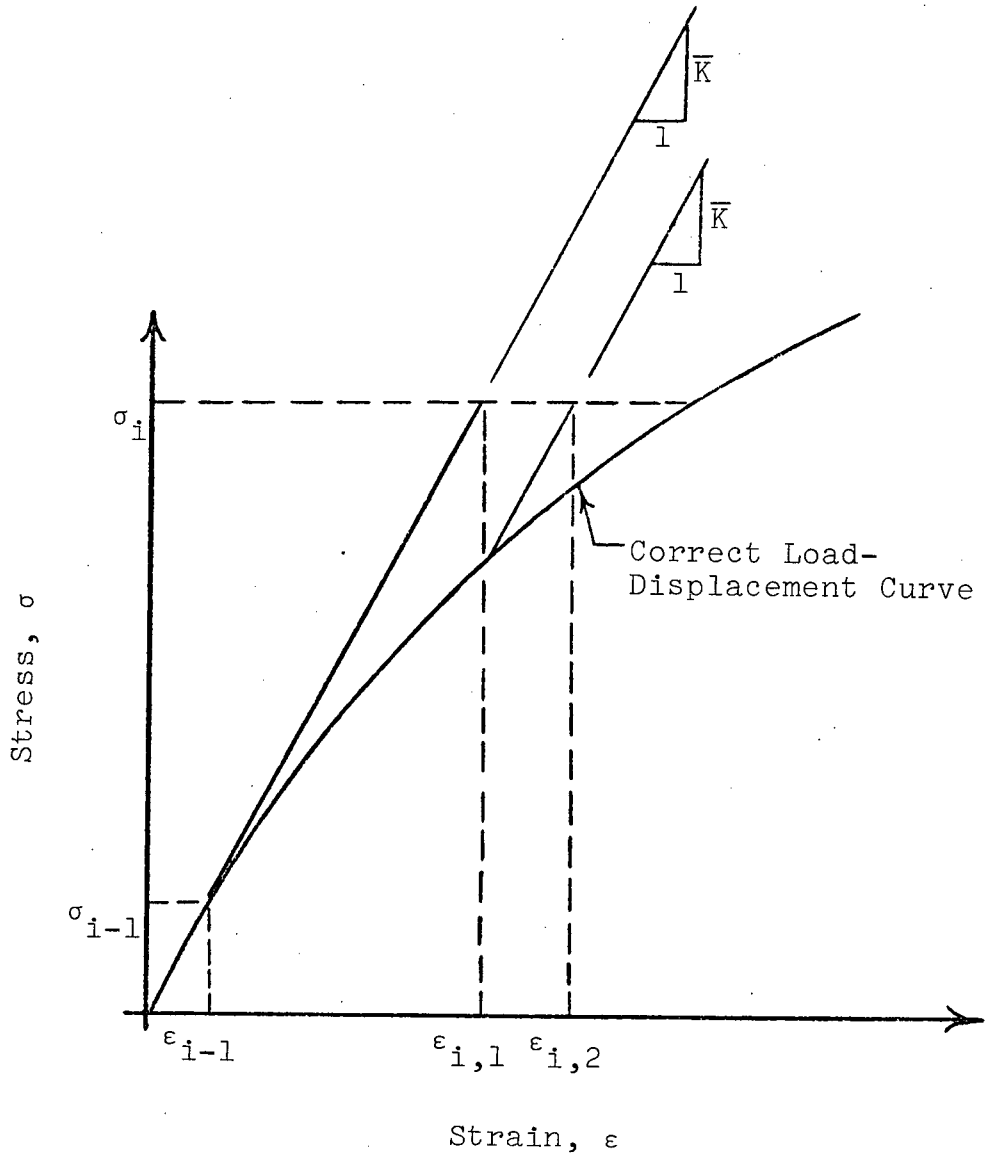

FIGURE 3 NEWTON-RAPHSON METHOD FOR THE ONE-DIMENSIONAL CASE

The process is continued until σ^e is small enough to be acceptable.

The Newton-Raphson method is readily modified for use in nonlinear analyses of the response of bodies to applied loadings. The initial estimates of the incremental nodal displacements, $\{\Delta q\}_{i,1}$, incremental strains, $\{\Delta\varepsilon\}_{i,1}$ and incremental element stresses, $\{\Delta\sigma\}_{i,1}$, are found as in section (2.2.1). The first estimates of the nodal displacements, $\{q\}_{i,1}$, element strains, $\{\varepsilon\}_{i,1}$, and element stresses, $\{\sigma\}_{i,1}$ at the end of the ith load increment are given by

$$\{q\}_{i,1} = \{q\}_{i-1} + \{\Delta q\}_{i,1} \tag{2-33}$$

$$\{\varepsilon\}_{i,1} = \{\varepsilon\}_{i-1} + \{\Delta\varepsilon\}_{i,1} \tag{2-34}$$

and

$$\{\sigma\}_{i,1} = \{\sigma\}_{i-1} + \{\Delta\sigma\}_{i,1} \tag{2-35}$$

Since $\{\sigma\}_{i,1}$ is an equilibrium stress vector for the end of the ith load increment,

$$\{\sigma\}_i = \{\sigma\}_{i,1} \tag{2-36}$$

The difference, $\{\sigma^e\}_{i,1}$, between $\{\sigma\}_i$ and the stresses specified by the stress-strain relation of the material for the strains, $\{\varepsilon\}_{i,1}$, is found using equation (2-26). The nodal correction forces corresponding to $\{\sigma^e\}_{i,1}$ are then found from equation (2-30). A correction, $\{\Delta q\}'_{i,1}$, to the nodal displacement vector, $\{q\}_{i,1}$ is then found by solving

$$[K_T]_i \{\Delta q\}'_{i,1} = \{Q^e\}_{i,1} \tag{2-37}$$

in which $[K_T]_i$ is the same global stiffness matrix used to obtain $\{\Delta q\}_{i,1}$. An improved estimate, $\{q\}_{i,2}$, of the nodal displacement vector is given by

$$\{q\}_{i,2} = \{q\}_{i,1} + \{\Delta q\}'_{i,1} \tag{2-38}$$

An improved estimate, $\{\varepsilon\}_{i,2}$, of the element strains is given by

$$\{\varepsilon\}_{i,2} = \{\varepsilon\}_{i,1} + \{\Delta\varepsilon\}'_{i,1} \tag{2-39}$$

in which $\{\Delta\varepsilon\}'_{i,1}$ is the vector of strains corresponding to $\{\Delta q\}'_{i,1}$. The difference, $\{\sigma^e\}_{i,2}$, between $\{\sigma\}_i$ and the stresses specified by the stress-strain relation of the material for the strains, $\{\varepsilon\}_{i,2}$, is found and the process is repeated until, on the nth iteration, $\{\sigma^e\}_{i,n}$ is small enough to be acceptable.

This method is called the "initial stress method" by Zienkiewicz (19) and the "residual stress method" by Nyak and Zienkiewicz (14).

This method has two advantages. First, the global stiffness matrix does not have to be changed during the iterative process. This saves considerable computational effort. Secondly, since the difference between the equilibrium stresses, $\{\sigma\}_i$, and the stresses specified by the stress-strain relation of the material for the calculated element strains is evaluated during each iteration, it is possible to specify explicitly the accuracy with which the stress-strain relation of the material is followed.

While the modified Newton-Raphson method is easily applied in problems in which a single known stress-strain curve is used, it is more difficult to apply to problems in which a family of stress-strain curves is used and a given point, within the body being analysed, follows a different stress-strain curve at different stages of loading. In such cases, one may have to make assumptions regarding the stress-strain behaviour in order to allow the calculation of the stresses which are compatible with both the stress-strain curves and the computed strains.

CHAPTER 3

STRESS-STRAIN RELATIONS

3.1 General Discussion of Stress-Strain Relations

In order to predict the deformations of soil structures under applied loadings, one needs a constitutive or stress-strain model for the soil. Because of the complex behaviour of soils, one finds it convenient to assume the behaviour of soils to be linear over small load increments. Therefore, one requires an incremental constitutive relation.

A possible constitutive relation for soils is the generalized form of Hooke's Law for a homogeneous elastic material. This is, in incremental form,

$$\begin{Bmatrix} \Delta\sigma_x \\ \Delta\sigma_y \\ \Delta\sigma_z \\ \Delta\tau_{xy} \\ \Delta\tau_{yz} \\ \Delta\tau_{zx} \end{Bmatrix} = \begin{bmatrix} D_{11} & D_{12} & D_{13} & D_{14} & D_{15} & D_{16} \\ D_{21} & D_{22} & D_{23} & D_{24} & D_{25} & D_{26} \\ \vdots & \vdots & \vdots & \vdots & \vdots & \vdots \\ \vdots & \vdots & \vdots & \vdots & \vdots & \vdots \\ \vdots & \vdots & \vdots & \vdots & \vdots & \vdots \\ D_{61} & D_{62} & D_{63} & D_{64} & D_{65} & D_{66} \end{bmatrix} \begin{Bmatrix} \Delta\varepsilon_x \\ \Delta\varepsilon_y \\ \Delta\varepsilon_z \\ \Delta\gamma_{xy} \\ \Delta\gamma_{yz} \\ \Delta\gamma_{zx} \end{Bmatrix}$$

or $$\{\Delta\sigma\} = [D]\{\Delta\varepsilon\} \qquad (3\text{-}1)$$

The constitutive or stress-strain matrix, [D], is symmetric and contains twenty-one independent elastic moduli. If this

general form of Hooke's Law were used as the constitutive model for a soil, it would be necessary to evaluate twenty-one different elastic moduli as functions of the state of stress or strain in the soil, which would be a rather formidable task.

If the soil is assumed to be isotropic as well as homogeneous and elastic, equation (3-1) becomes

$$\begin{Bmatrix} \Delta\sigma_x \\ \Delta\sigma_y \\ \Delta\sigma_z \\ \Delta\tau_{xy} \\ \Delta\tau_{yz} \\ \Delta\tau_{zx} \end{Bmatrix} = \begin{bmatrix} D_{11} & D_{12} & D_{13} & 0 & 0 & 0 \\ D_{21} & D_{22} & D_{23} & 0 & 0 & 0 \\ D_{31} & D_{32} & D_{33} & 0 & 0 & 0 \\ 0 & 0 & 0 & D_{44} & 0 & 0 \\ 0 & 0 & 0 & 0 & D_{55} & 0 \\ 0 & 0 & 0 & 0 & 0 & D_{66} \end{bmatrix} \begin{Bmatrix} \Delta\varepsilon_x \\ \Delta\varepsilon_y \\ \Delta\varepsilon_z \\ \Delta\gamma_{xy} \\ \Delta\gamma_{yz} \\ \Delta\gamma_{zx} \end{Bmatrix} \tag{3-2}$$

in which the constitutive matrix is symmetric and

$$D_{11} = D_{22} = D_{33}$$

$$D_{44} = D_{55} = D_{66}$$

and

$$D_{12} = D_{13} = D_{23}$$

The constitutive matrix for the isotropic homogeneous elastic material is defined by only two independent elastic moduli since D_{12} is a linear combination of D_{11} and D_{44}. Thus, by assuming that a soil is isotropic as well as homogeneous and elastic under small load increments, the number of moduli needed to model its stress-strain characteristics is reduced from twenty-one to only two. For this reason

soils are usually assumed to be isotropic.

While the assumption of isotropy saves considerable effort in modelling the stress-strain behaviour of a soil, it is not accurate for some soils.

The volumetric strain, ε_v, in any material is defined as

$$\varepsilon_v = \frac{dV}{V} \tag{3-3}$$

where dV is an infinitesimal change in the volume, V, of the element of the material. For an infinitesimal element of a material, the volumetric strain may be written in terms of the normal strains, ε_x, ε_y and ε_z as

$$\varepsilon_v = \varepsilon_x + \varepsilon_y + \varepsilon_z \tag{3-4}$$

Inspection of the constitutive relation, equation (3-2), for an isotropic homogeneous elastic material reveals that the normal strains are independent of the shear stresses. Shear stresses, therefore, do not cause volumetric strains in isotropic materials. The same is true for orthotropic materials.

For sands and overconsolidated clays, however, shear stresses are known to cause volumetric strains. Girijavallabhan and Reese (12) found that, for a dense sand, shear stresses may, in some cases, be more effective in producing volumetric strains than are hydrostatic stresses.

For sands and overconsolidated clays then, the assumption of isotropy is not correct. As a result, the

deformations predicted when one uses the assumption that these soils are isotropic as well as homogeneous and elastic will be somewhat in error especially when large shear stresses are involved. A more accurate model for the stress-strain properties of sands and overconsolidated clays would have to take the coupling between shear stresses and volumetric strains into account. This would require more independent elastic moduli. Despite its inaccuracy for sands and overconsolidated clays, the assumption of isotropy is usually made when modelling the stress-strain behaviour of any soil since it greatly reduces the effort necessary to produce a model.

If a soil is assumed to be an isotropic homogeneous elastic material for small load increments, two independent moduli are needed to define its stress-strain properties.

The moduli most commonly used are the tangent Young's modulus, E_t, the tangent shear modulus, G_t, the tangent bulk modulus, K_t, the tangent Poisson's ratio, ν_t, and the tangent constrained modulus, M_t. These are defined as follows:

$$E_t = \frac{\delta\sigma_i}{\delta\varepsilon_i} \tag{3-5}$$

$$G_t = \frac{\delta\tau_{ij}}{\delta\gamma_{ij}} \tag{3-6}$$

$$K_t = \frac{\delta\sigma_m}{\delta\varepsilon_v} \quad \text{where } \sigma_m = \frac{\sigma_x+\sigma_y+\sigma_z}{3} \tag{3-7}$$

$$\nu_t = \frac{\delta\varepsilon_i}{\delta\varepsilon_j} \tag{3-8}$$

and

$$M_t = \frac{\delta\sigma_i}{\delta\varepsilon_i} \text{ with } \varepsilon_j = \varepsilon_k = 0 \tag{3-9}$$

The bulk modulus, the shear modulus, Young's modulus and the constrained modulus must all be positive.

Any two of the moduli defined by equations (3-5) to (3-9) may be regarded as independent. The shear, bulk and constrained moduli are related to Young's modulus and Poisson's ratio by the following equations:

$$G_t = \frac{E_t}{2(1+\nu)} \tag{3-10}$$

$$K_t = \frac{E_t}{3(1-2\nu)} \tag{3-11}$$

and

$$M_t = \frac{E_t(1-\nu)}{(1+\nu)(1-2\nu)} \tag{3-12}$$

if the soil is isotropic.

From equation (3-11), it follows that Poisson's ratio may not be greater than 0.5 since this would result in a negative bulk modulus.

Desai and Abel (4) give the following constitutive matrices, [D], for an isotropic homogeneous elastic material:

in terms of E_t and ν_t,

$$D_{11} = D_{22} = D_{33} = \frac{E_t(1-\nu_t)}{(1+\nu_t)(1-2\nu_t)}$$

$$D_{12} = D_{13} = D_{23} = \frac{\nu_t E_t}{(1+\nu_t)(1-2\nu_t)}$$

$$D_{44} = D_{55} = D_{66} = \frac{E_t}{2(1+\nu_t)}$$

and in terms of G_t and K_t,

$$D_{11} = D_{22} = D_{23} = K_t + 4/3\ (G_t)$$

$$D_{12} = D_{13} = D_{23} = K_t - 2/3\ (G_t)$$

$$D_{44} = D_{55} = D_{66} = G_t$$

Drnevich (7) gives the following constitutive matrix in terms of M_t and G_t:

$$D_{11} = D_{22} = D_{33} = M_t$$

$$D_{12} = D_{13} = D_{23} = M_t - 2G_t$$

$$D_{44} = D_{55} = D_{66} = G_t$$

The choice of which two moduli one uses to define a soil's stress-strain properties will depend upon the convenience of the test necessary to determine them and the degree of certainty with which they may be determined.

Small uncertainties in the value of Poisson's ratio may cause large uncertainties in the elements of the constitutive matrix, $[D]_e$. For example, if the value of Poisson's ratio is 0.48, the bulk modulus is eight and one-third times the value of Young's modulus. But if the value of Poisson's ratio is one-half, the bulk modulus is

infinite. Uncertainties in Poisson's ratio are, however, less important when it is smaller.

Since soils are generally nonlinear in their stress-strain behaviour, the moduli used to define their constitutive relations have to be determined as functions of the stress or strain state.

3.2 Experimental Studies

Duncan and Chang (9) proposed that the constitutive matrix, [D], for a soil be written in terms of the tangent value of Young's modulus, E_t, and the tangent value of Poisson's ratio, ν_t and presented data on Young's modulus and Poisson's ratio for sands and clays. They found that if drained or undrained compressive triaxial tests are conducted at constant values of the minor principal stress, σ_3, the stress-strain relations observed for primary loading of soils may be represented by hyperbolic equations of the form

$$(\sigma_1 - \sigma_3) = \frac{\varepsilon_1}{\frac{1}{E_i} + \frac{\varepsilon_1}{(\sigma_1 - \sigma_3)_{ult}}} \qquad (3\text{-}13)$$

in which $(\sigma_1 - \sigma_3)$ is the deviator stress, ε_1 is the strain in the direction of the major principal stress, σ_1, and $(\sigma_1 - \sigma_3)_{ult}$ is the asymptotic value of the deviator stress (Figure 4). E_i is the initial value of the modulus and can be expressed as

$$E_i = K\, p_a \left(\frac{\sigma_3}{p_a}\right)^n \qquad (3\text{-}14)$$

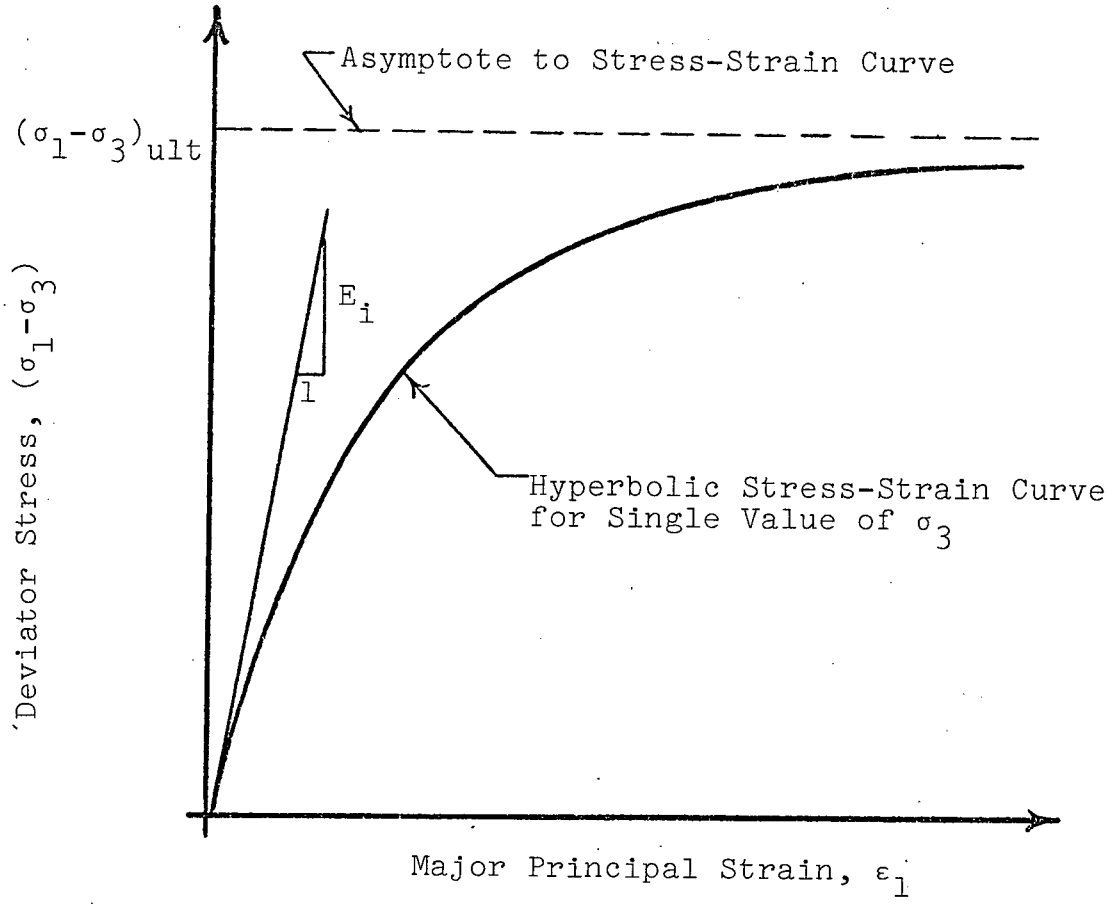

FIGURE 4 HYPERBOLIC STRESS-STRAIN CURVE

in which K is a dimensionless quantity called the modulus number, p_a is atmospheric pressure, and n is a dimensionless number called the modulus exponent. The value of $(\sigma_1 - \sigma_3)_{ult}$ is always greater than the deviator stress at failure, $(\sigma_1 - \sigma_3)_f$, which may be defined by the Mohr-Coulomb failure criterion as

$$(\sigma_1 - \sigma_3)_f = \frac{2\ c\ \cos\phi + 2\ \sigma_3\ \sin\phi}{1 - \sin\phi} \tag{3-15}$$

in which c is the cohesion intercept of the soil and ϕ is the angle of internal friction of the soil (Figure 5).

Duncan and Chang (9) expressed the relationship between $(\sigma_1 - \sigma_3)_{ult}$ and $(\sigma_1 - \sigma_3)_f$ by the equation

$$(\sigma_1 - \sigma_3)_f = R_f\ (\sigma_1 - \sigma_3)_{ult} \tag{3-16}$$

where R_f is known as the failure ratio. Typical values of R_f range from about 0.6 to 0.95.

The tangent value of Young's modulus, E_t, for triaxial tests conducted at a fixed value of σ_3 may be defined as

$$E_t = \frac{d(\sigma_1 - \sigma_3)}{d\ \varepsilon_1} \tag{3-17}$$

Using equations (3-13), (3-14), (3-15), (3-16) and (3-17), Duncan and Chang (9) expressed the tangent Young's modulus as a function of the stresses by the equation

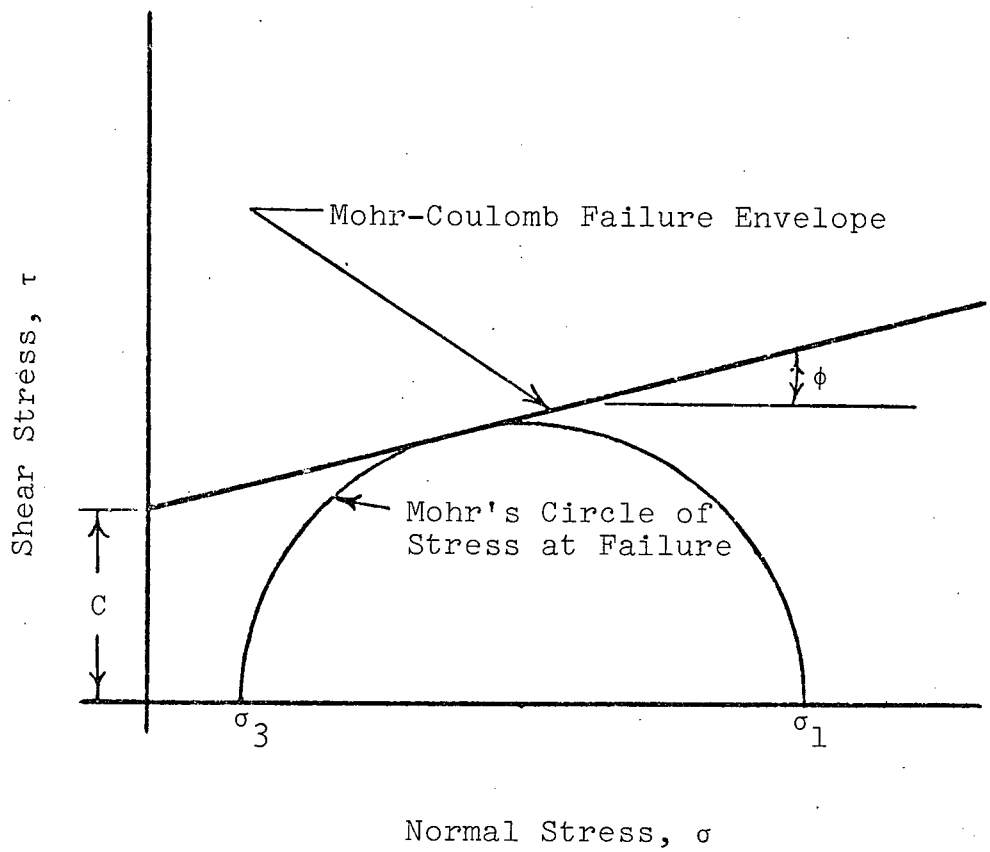

FIGURE 5 MOHR-COULOMB FAILURE CRITERION

$$E_t = \left[1 - \frac{R_f(1-\sin\phi)(\sigma_1-\sigma_3)}{2c\cos\phi+2\sigma_3\sin\phi}\right]^2 K\, p_a\left(\frac{\sigma_3}{p_a}\right)^n \tag{3-18}$$

The tangent value of Poisson's ratio is defined as the instantaneous rate of change of radial strain with respect to axial strain in the triaxial test.

At a constant value of σ_3 the tangent value of Poisson's ration, ν_t, for sands and clays is given by

$$\nu_t = \frac{G - F\log(\sigma_3/p_a)}{1 - \left[\dfrac{d(\sigma_1 - \sigma_3)}{K\, p_a\left(\dfrac{\sigma_3}{p_a}\right)^n \left[1 - \dfrac{R_f(\sigma_1-\sigma_3)(1-\sin\phi)}{2c\cos\phi+2\sigma_3\sin\phi}\right]}\right]} \tag{3-19}$$

in which G is the value of ν_t when $\sigma_3 = p_a$, F is the decrease in ν_t for a tenfold increase in σ_3 and d is the rate of increase of ν_t with strain and all other parameters are the same as in equation (3-18). For undrained conditions G is one-half and F and d are both zero.

Domaschuk and Wade (6) proposed that the constitutive matrix, [D], for a soil be written in terms of the tangent shear modulus, G_t, and the tangent bulk modulus, K_t, and they presented data on the bulk and shear moduli of sands.

In order to investigate the behaviour of a sand in shear, they performed a number of drained triaxial compression tests at constant values of the mean normal stress,

σ_m, on sands of various initial relative densities. These tests yielded data on the relationships between the resultant deviatoric stress, S_d, given by

$$S_d = \left((\sigma_1-\sigma_m)^2 + (\sigma_2-\sigma_m)^2 + (\sigma_3-\sigma_m)^2\right)^{\frac{1}{2}} \qquad (3\text{-}20)$$

and the resultant deviatoric strain, ε_d, given by

$$\varepsilon_d = \left((\varepsilon_1-\varepsilon_m)^2 + (\varepsilon_2-\varepsilon_m)^2 + (\varepsilon_3-\varepsilon_m)^2\right)^{\frac{1}{2}} \qquad (3\text{-}21)$$

in which ε_m is the mean normal strain. The general form of these relationships was expressed by the hyperbolic stress-strain relation

$$S_d = \frac{\varepsilon_d G_i}{1 + b\varepsilon_d G_i} \qquad (3\text{-}22)$$

in which G_i is the initial value of the tangent shear modulus, defined as the instantaneous rate of change of S_d with respect to ε_d, and b is the inverse of the asymptotic value of S_d. Both G_i and b were found to depend upon the initial relative density of the sand and the mean normal stress at which the test was performed.

By differentiating equation (3-22) with respect to ε_d, Domaschuk and Wade (6) arrived at the following expression for the tangent shear modulus

$$G_t = G_i(1 - b\ S_d)^2 \qquad (3\text{-}23)$$

In order to investigate the bulk modulus of sands, Domaschuk and Wade (6) performed a number of isotropic consolidation tests on sands of various initial relative

densities and plotted curves of the mean normal stress, σ_m, versus the volumetric strain, ε_v. They found the following relationship between the tangent bulk modulus, K_t, defined as the instantaneous rate of change of σ_m with respect to ε_v, and the mean normal stress, σ_m

$$K_t = K_i + m\sigma_m \tag{3-24}$$

in which K_i is the value of the tangent bulk modulus when ε_v is zero and m is the rate of change of K_t with σ_m. Both K_i and m depend upon the initial relative density of the sand.

For a sand of a given relative density, the relationship between K_t and σ_m is a bi-linear one which may be expressed by two equations from the form of equation (3-24), each of which is appropriate to a range of values of σ_m.

Domaschuk and Valliappan (5) extended the work of Domaschuk and Wade (6) to clays. They found that the relationship between the resultant deviatoric stress and the deviatoric strain for drained triaxial compression tests was of the same form for clays as that for sands. Consequently, the relationship between the tangent shear modulus and the resultant deviatoric stress was also given by equation (3-23). The values of G_i and b for a clay are related to the initial void ratio of the clay, its preconsolidation pressure and the mean normal stress at which the

test was conducted.

The tangent bulk modulus, K_t, of a clay was found to be related to a normalized volumetric strain, ε_{vn}, by the relationship

$$K_t = K_i \left(1 + N \varepsilon_{vn}^{n-1}\right) \tag{3-25}$$

in which K_i is the initial value of the tangent bulk modulus and N is a number which indicates the rate of increase of K_t with that of ε_{vn}. The initial bulk modulus is given by

$$K_i = \sigma_{mc}/\varepsilon_{vc} \tag{3-26}$$

in which σ_{mc} and ε_{vc} are characteristic values of the isotropic stress and the volumetric strain at which the initial tangent to the stress-strain curve and a straight line approximation to the final portion of the stress-strain curve intersect. When n is infinite, equation (3-25) expresses an elastoplastic stress-strain curve. According to Domaschuk and Valliappan (5), σ_{mc}, ε_{vc} and N were found by a method of least squares adjustment described by Deming (3). The normalized volumetric strain, ε_{vn}, is given by

$$\varepsilon_{vn} = |\varepsilon_v/\varepsilon_{vc}| \tag{3-27}$$

Drnevich (7) proposed the use of the constrained modulus, M, in nonlinear analyses of problems which approximate one-dimensional compression. This would be used together with another modulus such as the shear modulus to define the constitutive matrix, [D]. He performed a number

of one-dimensional compression tests on sands and plotted the data as the axial stress, σ_1, versus the axial strain, ε_1. The results were represented by hyperbolic equations of the form

$$\sigma_1 = \frac{M_i \ \varepsilon_1}{1 - \frac{\varepsilon_1}{\varepsilon_m}} \tag{3-28}$$

in which M_i is the initial value of the constrained modulus, defined as the instantaneous rate of change of σ_1 with respect to ε_1, and ε_m is the asymptotic value of the strain.

By differentiating equation (3-28) with respect to ε_1, Drnevich (7) found the following relationship between the tangent constrained modulus, M_t, and ε_1

$$M_t = M_i \frac{\varepsilon_m^2}{(\varepsilon_m - \varepsilon_1)^2} \tag{3-29}$$

By solving equation (3-29) for ε and substituting the result into equation (3-28), Drnevich (7) obtained the following expression for the tangent constrained modulus in terms of σ

$$M_t = M_i \left[\frac{(1+\sigma_1)}{\varepsilon_m \ M_i} \right]^2 \tag{3-30}$$

3.3 Limitations of Stress-Strain Relations

The stress-strain relations discussed in section (3.2) have certain limitations. First, they are all based upon the assumption of isotropic elastic behaviour and thus none of them accounts for volume changes due to shear even though volume changes due to shear may have occurred in the tests used to establish them. The use of these stress-strain relations, therefore, may not be satisfactory when dealing with soils which develop significant volume changes due to shear strains.

Secondly, since the expressions discussed in section (3.2), which relate the values of the moduli to the state of stress, are based upon elastic theory, they are not applicable beyond the point of yield when soils act more like plastic materials.

Thirdly, for soils, different stress-paths to the same state of stress may lead to different values of a particular elastic modulus.

Using the percentage of the strength of the soil that is mobilized to resist an applied loading as the definition of stress-level, Lade and Duncan (13) have made a classification of loadings into primary loading which produces monotonically increasing stress-levels above those previously experienced by the soil, unloading which produces decreasing stress-levels and reloading which produces increasing stress-levels below those previously experienced

by the soil.

The stress-strain behaviour of cohesionless soils in primary loading is different from that in unloading or reloading since the strains induced during primary loading are partially irrecoverable. Lade and Duncan (13) found that this difference generally increased as the stress-level increased. Duncan and Chang (9) found similar results for clays.

Lade and Duncan (13) concluded from a review of published data that, for cohesionless soils, any two stress-paths involving only primary loading would produce nearly the same strains in going from one state of stress to another. However, stress-paths involving any unloading or reloading would produce smaller strains than a stress-path involving only primary loading in going from one state of stress to another. For example, in Figure (6), stress-path P-1, which involves only primary loading, would produce larger strains than would stress-path P-2, which involves some unloading and reloading, in going from the state of stress represented by point A to that represented by point B.

Duncan and Chang (10), in their discussion of their expressions for the tangent values of Young's modulus (equation (3-18)) and Poisson's ratio (equation (3-19)), stated that their expressions, with parameters obtained from triaxial compression tests performed at constant values of the minor principal stress, were unable to predict accurately

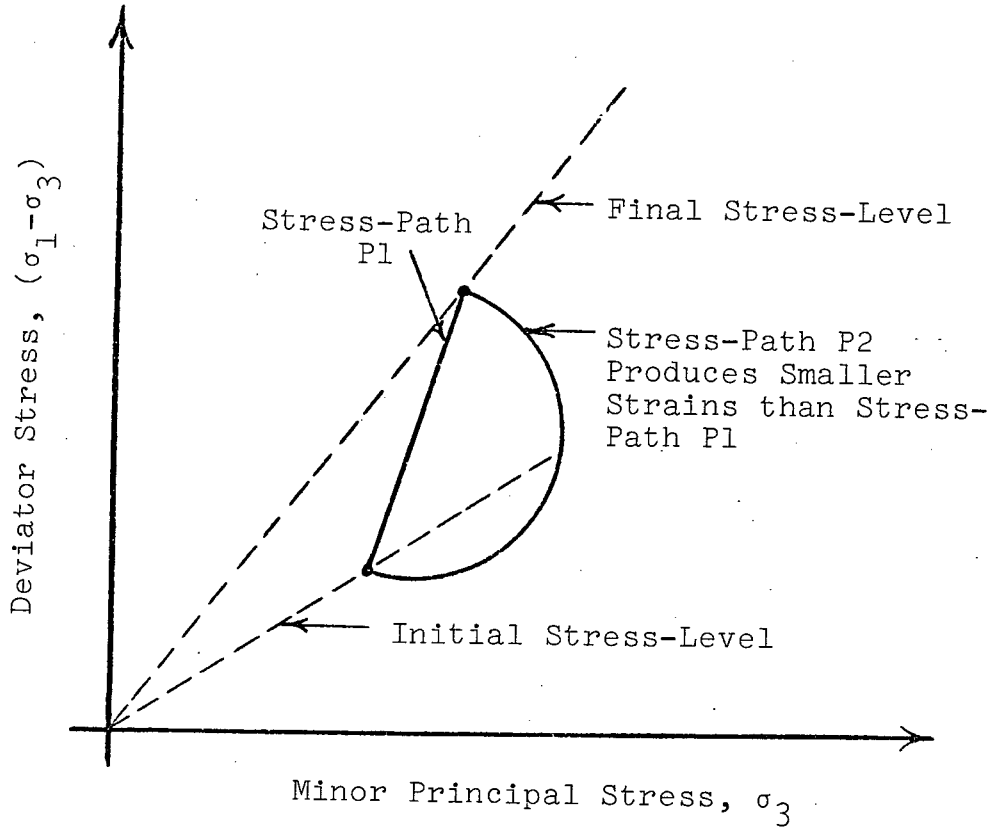

FIGURE 6 TWO STRESS-PATHS WHICH YIELD DIFFERENT STRAINS FOR THE SAME STRESS INCREMENT

the strains induced in a triaxial test specimen of a uniform fine sand of low relative density when the principal stresses were increased in such a way that the percentage of available soil strength mobilized was constant (that is, so that the stress-level was constant).

Yudhbir and Varadarajan (18) conducted stress controlled, drained triaxial tests on normally consolidated clays for several stress-paths. The stress-paths were as follows:

(a) σ_1 increasing with σ_3 constant;

(b) σ_1 increasing with constant mean normal stress;

(c) σ_1 constant with σ_3 decreasing;

(d) isotropic decrease of normal stresses.

They evaluated the tangent values of Young's modulus and Poisson's ratio using the appropriate Hooke's Law expression for isotropic materials for each stress-path. In the case of stress-path (b), however, only the tangent shear modulus could be evaluated directly and an estimate of Poisson's ratio was used to estimate the tangent value of Young's modulus.

Yudhbir and Varadarajan (18) found that the variation of the initial tangent value of Young's modulus with consolidation pressure could be expressed by equations of the same form as equation (3-14) but that the values of the modulus number, K, and the modulus exponent, n, were different for each of the different stress-paths; K varied

from sixteen for stress-path (a) to one-hundred and five for stress-path (d) while n varied from about one-half for stress-path (c) to about nine-tenths for stress-path (a). The tangent value of Young's modulus, E_t, at any stage of a test conducted with a single stress-path, was expressed as a function of the stress-level, S, (fraction of strength mobilized) by an equation of the form

$$E_t = (1 - R_f S)^2 E_i \tag{3-31}$$

in which E_i is the initial tangent Young's modulus and R_f is defined as in equation (3-16). The value of R_f depended upon the stress-path followed and ranged from about six-tenths for stress-path (a) to just over nine-tenths for stress-path (c).

Yudhbir and Varadarajan (18) concluded that the effect of stress-path on the stress-strain relationship and on the tangent value of Young's modulus at a particular state of stress is very significant for normally consolidated clays.

Corotis, Farzin and Krizek (2) conducted triaxial compression tests on two soils, A, a mixture of coarse to very fine sand containing about five percent silt, and B, a mixture of sand, silt and clay. The tests were conducted using stress-paths with $d\sigma_3/d\sigma_1$ varying from zero to one. Only one value of $d\sigma_3/d\sigma_1$ was used in each test. They found that the stress-path used affected the relationships between the state of stress and both Young's modulus

and Poisson's ratio for both of the soils tested.

It is apparent from all these studies that the stress-path followed during loading may have a significant effect on the stress-strain relations and elastic moduli of soils. The expressions for the elastic moduli of soils and the stress-strain relations of soils may, therefore, be said to be correct only for the stress-paths for which they were obtained.

3.4 Material Behaviour After Yield

Although the behaviour of soils after yield is generally that of a plastic material, Duncan (8) reports that many authors deal with soils after yield as soft elastic materials. This simplifies the modelling of soil stress-strain behaviour.

Duncan and Chang (9) used Young's modulus, as given by equation (3-18) together with a constant value of Poisson's ratio, to define the stress-strain behaviour of a sand in an analysis of the load-deformation response of a buried strip footing. They simulated yield by reducing Young's modulus to a very small value.

As may be seen from equations (3-10) and (3-11), the simple reduction of the value of Young's modulus at yield results in a proportionate reduction of both the shear modulus and the bulk modulus. However, according to Duncan (personal correspondence), the bulk modulus

immediately after yield should not be very different from that immediately prior to yield. The practice of simply reducing Young's modulus to some arbitrary small value at yield is, therefore, not acceptable since it implies that the ability of the soil to resist changes in hydrostatic stress is greatly reduced.

It is, however, possible to change the values of both Poisson's ratio and Young's modulus at yield in such a way that the value of the bulk modulus remains unchanged even though the shear modulus is greatly reduced.

Consider the case in which Young's modulus immediately before yield is R times that immediately after yield, and the value of Poisson's ratio immediately before yield is ν_1. The value of Poisson's ratio immediately after yield, ν_2, which will maintain the value of the bulk modulus at that immediately prior to yield is given by

$$\nu_2 = \frac{R - 1 + 2\nu_1}{2R} \tag{3-32}$$

For example, if Young's modulus immediately after yield is set equal to one-thousandth of that immediately prior to yield and the value of Poisson's ratio prior to yield was 0.45, then the value of Poisson's ratio after yield would have to be increased to 0.4995 in order for the bulk modulus to remain unchanged.

If ν_2 is chosen using equation (3-32), the value of the shear modulus immediately after yield is then

B times that immediately prior to yield, where B is given by

$$B = \frac{1 + \nu_1}{R + \frac{R - 1 + 2\nu_1}{2}} \tag{3-33}$$

For the above example then, choosing ν_2 according to equation (3-32) would give a value of the shear modulus after yield equal to 0.00097 times that prior to yield.

According to Duncan (8), when using a computer to perform nonlinear analyses, it is common practice to limit Poisson's ratio to values less than about 0.49 in order to avoid computational difficulties. Inspection of equation (3-32) shows, however, that even if the value of Poisson's ratio were zero prior to yield, the value of Poisson's ratio after yield must be 0.495 in order to leave the bulk modulus unchanged while reducing Young's modulus by a factor of one-hundred at yield. Therefore, limiting Poisson's ratio to values of not more than 0.49 will lead to a reduction of the bulk modulus when Young's modulus is reduced at yield. It would be desirable to use equation (3-32) to select values of Poisson's ratio for use after yield. However, doing this may lead to computational difficulties since the bulk modulus tends to infinity as Poisson's ratio approaches one-half.

If the shear and bulk moduli are used as the independent elastic constants these difficulties do not occur for compressible soils. One may simply reduce the

shear modulus at yield and maintain the bulk modulus at the value it had prior to yield.

CHAPTER 4

PROBLEMS IN NONLINEAR FINITE ELEMENT ANALYSIS OF DEFORMATIONS IN SOIL BODIES

4.1 General Discussion of Nonlinear Finite Element Analysis of Deformations in Soil Bodies

4.1.1 Common Assumptions

In order to perform incremental nonlinear finite element analyses of soil bodies, certain assumptions are commonly made.

The displacement field for the finite elements may be assumed to be linear, quadratic, or of a higher order. For any assumed displacement field, the stiffness of the finite element mesh used to model a body will be an upper bound to the actual stiffness of that body if the correct constitutive model for the material is used and the following conditions (Desai and Abel (4)) are met:

1. The displacements are continuous within the elements and compatible between adjacent elements.
2. The displacement field allows rigid body displacements of the finite elements.
3. The displacement field allows constant strain states in the finite elements. That is, the displacement field must contain linear terms.

If the above conditions are met, the stiffness of the finite element mesh may be made closer to that of the body it represents by using finer subdivisions of the finite element mesh (Desai and Abel (4)).

Brebbia and Connor (1) compared the accuracy of constant strain triangular elements with that of higher order elements in the linear analysis of the response of a cantilever beam to loading. It was found that, for meshes of the same number of finite elements, those which used higher order elements gave more accurate stresses and deflections. For meshes with the same number of unknowns, those with the higher order elements gave better results. The same trends were found for rectangular elements.

Finn and Miller (11) state that their experience has been that one linear strain triangular element is roughly equivalent to six to ten constant strain triangular elements for stress computation. They report that the constant strain triangular element is even less efficient relative to the higher order elements in nonlinear analyses. They found that, in elastic-plastic analyses, the use of constant strain elements could prevent slip deformations along yielded elements.

Another common assumption is that the strains and displacements occurring during an analysis are small. This means that only linear terms are needed in the relationships between strains and displacements (see Desai and

Abel (4)). Also, it means that the initial geometry of the body may be used throughout the analysis.

It is also commonly assumed (2,5,6,7,8,9,10,11, 12,17,18) that soils are isotropic, elastic materials. This means that only two elastic moduli are needed to determine the stress-strain equations of soils. As explained in Chapter Three, however, the assumption of isotropy is not correct for soils which are susceptible to volume changes due to shear.

In order to allow the determination of the appropriate values of the elastic moduli at any stage of an incremental analysis, it is commonly assumed that the tangent moduli of soils are functions only of the existing state of stress. As pointed out in section (3.3), however, the moduli are also functions of stress-path.

Duncan and Chang (9) pointed out that it is desirable to relate the values of a soil's tangent moduli to stresses since these are usually more accurately known at any stage of an analysis than are the strains.

4.1.2 Method of Incremental Analysis

As was shown in Chapter 2, several methods of incremental nonlinear analysis are available. Any of these methods may be used for soils if the appropriate stress-strain relations are known.

In many nonlinear problems, different stress-paths

are followed by the soil in different parts of the soil mass at the same time. Moreover, if local failures occur within the soil mass, the stress-path followed at a particular point within the soil mass may be different at different stages of loading. In such cases, it would be necessary to use stress-strain relations which include all possible stress-paths if one wished to ensure that the stress-strain relations used are appropriate to the stress-paths followed. Such general stress-strain relations, however, do not exist for soils and one uses a family of stress-strain curves derived from tests performed with stress-paths other than those followed in the problem of interest. During the analysis of the problem, a point within the soil mass goes from one stress-strain curve in the family to another.

The use of families of stress-strain curves as described above makes difficult the use of methods such as the modified Newton-Raphson method or the application of correction forces, which are very useful in problems involving a unique stress-strain curve. In order to use these methods, one would have to make assumptions with regard to the stress-strain behaviour of the material in order to calculate the stresses which are compatible with both the stress-strain curves and the computed strains. For example, if the stress-strain curves used were described by equation (3-13), one might assume that Poisson's ratio had a constant value in order to find the correct ratio of the major and

minor principal stresses and solve equation (3-13) for them.

In analyses of problems in which the stress-paths followed are not those used to establish the stress-strain relations available, the best that one may do is to assume that the elastic moduli are functions only of the existing state of stress, and are given by equations derived from the stress-strain relations. Methods such as the one iteration per load increment method, described in section (2.2.1), or the iteration method using a convergence criterion, described in section (2.2.2), may then be used to perform incremental analyses. These methods do not require the calculation of the correct stresses for given strains. When using these methods, however, one may not exercise direct control over the errors which arise from the fact that the soil's stress-strain behaviour is actually nonlinear over the load increments used.

Intuitively, one feels that better agreement between the stress-strain curves generated using the one iteration per load increment method or iterations using a convergence criterion and the true stress-strain relations of the soil, may be obtained by decreasing the size of the load increments used, provided that the equations used to relate the tangent moduli to the state of stress are correct. However, since the expressions used to relate the tangent moduli of the soil to the state of stress do not take stress-paths into account, one does not know whether

or not the reduction of the size of the load increments will cause convergence to the correct result in problems with stress-paths other than those used to establish the expressions.

4.2 Numerical Studies

Yudhbir and Varadarajan (18) performed nonlinear finite element analyses for a retaining wall-soil system in which the wall rotated about its base away from the soil. The soil was a sedimented clay.

Constant strain triangular elements were used in the finite element mesh which represented the soil. The lower boundary of the mesh was at the same level as the base of the wall which was ten feet high. All nodes on the lower boundary of the mesh were assumed to be fixed. Wall rotation was simulated by the horizontal movement of the nodes adjacent to it. These nodes were assumed to be fixed to the wall.

The tangent values of Young's modulus were related to the state of stress by equation (3-18). In order to assess the importance of the effect of the stress-path used in evaluating the parameters in equation (3-18) on the results of the analysis, sets of parameters were evaluated using triaxial tests for two different stress-paths;

(a) σ_1 increasing with σ_3 constant, and

(b) σ_3 decreasing with σ_1 constant.

These stress-paths were chosen to bound the stress-paths followed in the problem.

The initial major and minor principal stresses in the clay at a depth h below the top of the wall were assumed to be

$$\sigma_1' = \gamma h \tag{4-1}$$

and

$$\sigma_3' = K_o \sigma_1' \tag{4-2}$$

in which σ_1' is the major principal effective stress, σ_3' is the minor principal effective stress, γ is the unit weight of the clay, and

$$K_o = 1 - \sin\phi' \tag{4-3}$$

in which ϕ' is the angle of internal friction for effective stress analysis of the clay.

Two analyses of the soil-wall system were carried out. In one, the data from the triaxial tests performed with stress-path A were used to relate Young's modulus to the state of stress; in the other, the data from the triaxial tests performed with stress-path B were used. In both analyses plane strain conditions were assumed.

Yudhbir and Varadarajan (18) plotted the predicted horizontal pressures at the soil-wall interface versus depth for each of the analyses. The predicted horizontal pressures at any depth were found to vary significantly with the stress-path used. The horizontal pressures predicted for a wall rotation of 0.006 radians using data

from stress-path A were higher at all depths than those predicted using data from stress-path B. The difference was as much as twenty percent.

Duncan and Chang (9) analysed the load-deformation response of a rectangular footing measuring 12.44 inches by 2.44 inches in plan and buried at a depth of twenty inches in Chatahoochee River sand. Constant strain quadrilateral elements were used in a plane strain analysis.

The relationship between the tangent value of Young's modulus and the state of stress was expressed by equation (3-18) up to the point of failure as defined by the Mohr-Coulomb failure criterion. The parameters used in equation (3-19) were found from three triaxial compression tests conducted at fixed values of the minor principal stress. Poisson's ratio was assumed to have a constant value of 0.35. The value of Young's modulus was arbitrarily reduced to ten pounds per square foot after failure.

The predicted behaviour of the footing under vertical loading was compared with that observed in a model test of the footing. The observed and predicted failure loads for the footing-soil system were nearly identical. However, the predicted average footing pressures associated with a given settlement were as much as fifty percent higher than those observed in the model test prior to failure. The predicted average footing pressures after failure were lower than those observed in the model test with the

difference increasing with increasing settlement.

The writer performed several incremental nonlinear analyses of the behaviour of a sand beneath a six inch wide surface strip footing subjected to vertical loading. The finite element program used was NONLIN, a program developed at the University of British Columbia. This program is designed to perform incremental nonlinear analyses for problems involving small strains using any compatible stress-strain subroutines supplied by the user. The program uses six node linear strain triangular elements. The stiffness matrix for this element is derived in Appendix 1.

The state of stress resulting from any loading would normally vary across a linear strain triangular element. The values of the tangent moduli would, therefore, vary across this element for a nonlinear material. However, NONLIN uses only one set of two moduli, based on the state of stress at the element centroid, for the entire element.

The writer developed subroutines based upon earlier work done by Roy (15) in order to use the hyperbolic stress-strain relations of Duncan and Chang (9) with the computer program NONLIN. These subroutines are presented in Appendix 2. The subroutines use equations (3-18) and (3-19) to relate the tangent values of Young's modulus and Poisson's ratio to the state of stress, up to the point of yield as defined by the Mohr-Coulomb failure criterion.

The tangent values of Young's modulus and Poisson's ratio are then converted to tangent values of the bulk and shear moduli for use with NONLIN.

The parameters used in equations (3-18) and (3-19) for the analyses performed were those presented by Wong and Duncan (17) for Sacramento River sand with a relative density of thirty-eight percent. These parameters were obtained from drained triaxial tests conducted at constant values of the minor principal stress and are as follows:

unit weight, γ = 89.5 pounds per cubic foot

angle of internal friction, ϕ = 35.0 degrees

cohesion intercept, c = 0.0 pounds per cubic foot

modulus number, k = 430

modulus exponent, n = 0.27

failure ratio, R_f = 0.84

Poisson's ratio parameter G = 0.42

Poisson's ratio parameter F = 0.21

Poisson's ratio parameter d = 2.9

The incremental analyses were carried out as described in section (2.2.1) using one iteration and no convergence criterion.

The finite element mesh used to model the footing-soil system is shown in Figure (7). One-half of a six inch wide rigid surface strip footing was represented by maintaining equal vertical displacements of the nine nodes

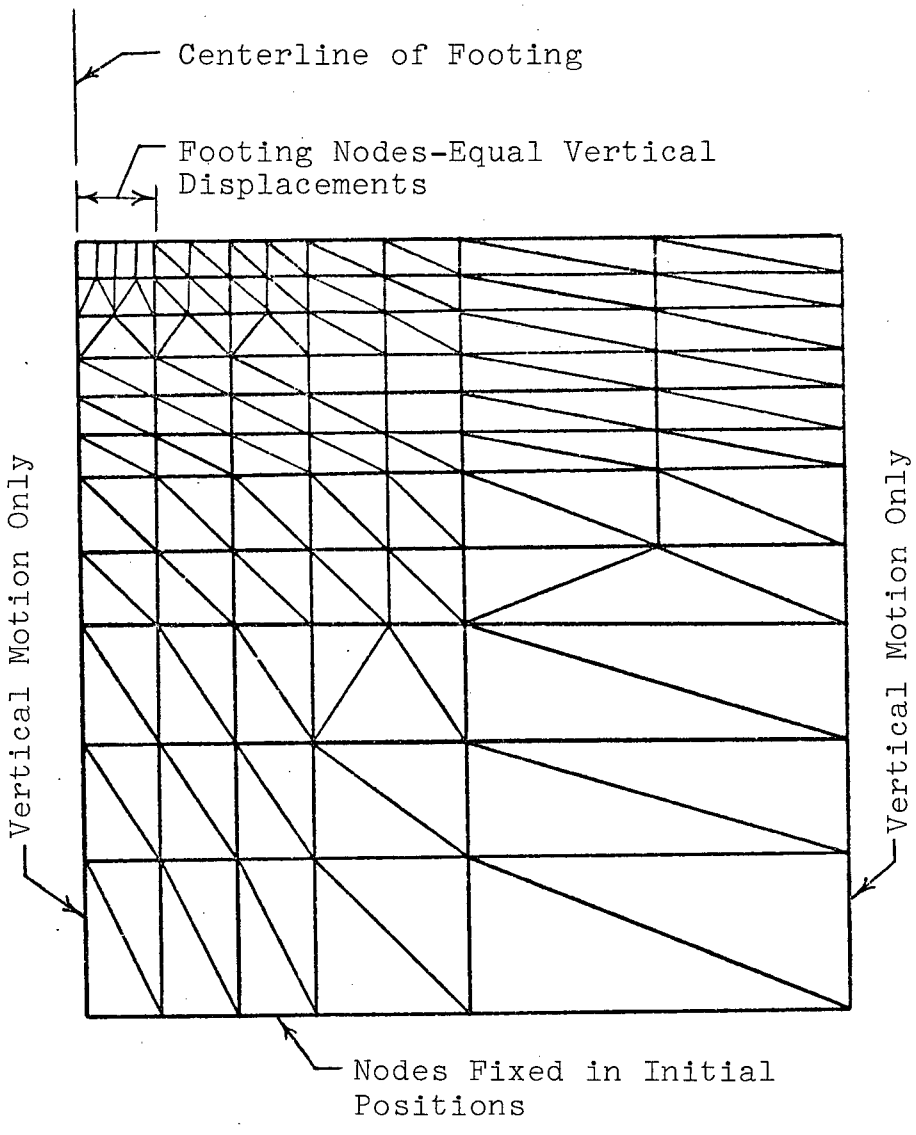

FIGURE 7 FINITE ELEMENT MESH

closest to the left hand edge on the upper surface of the mesh, during loading. In order to simulate a perfectly rough footing base, these nodes were not allowed to move horizontally. The nodes on the sides of the mesh were allowed only vertical motion. The nodes on the base of the finite element mesh were assumed to be fixed in their initial positions.

The initial stresses at the centroids of the finite element mesh were assumed to be given by equations (4-1) and (4-2) with h measured from the top of the finite element mesh. The coefficient of lateral earth pressure at rest, K_o, was taken to be 0.426 for the Sacramento River sand.

A set of analyses in which the tangent shear modulus was reduced to a small value at yield and the value of the tangent bulk modulus was kept the same after yield as that immediately prior to yield was performed. This approach is as suggested in section (3-4) by the writer.

The footing load-settlement curves predicted, using different size load increments in this set of analyses, are shown in Figures (8) and (9). Those shown in Figure (8) are for analyses in which the shear modulus of the sand was reduced to one-hundred pounds per square foot at yield while those shown in Figure (9) are for analyses in which the shear modulus of the sand was reduced to five pounds per square foot at yield.

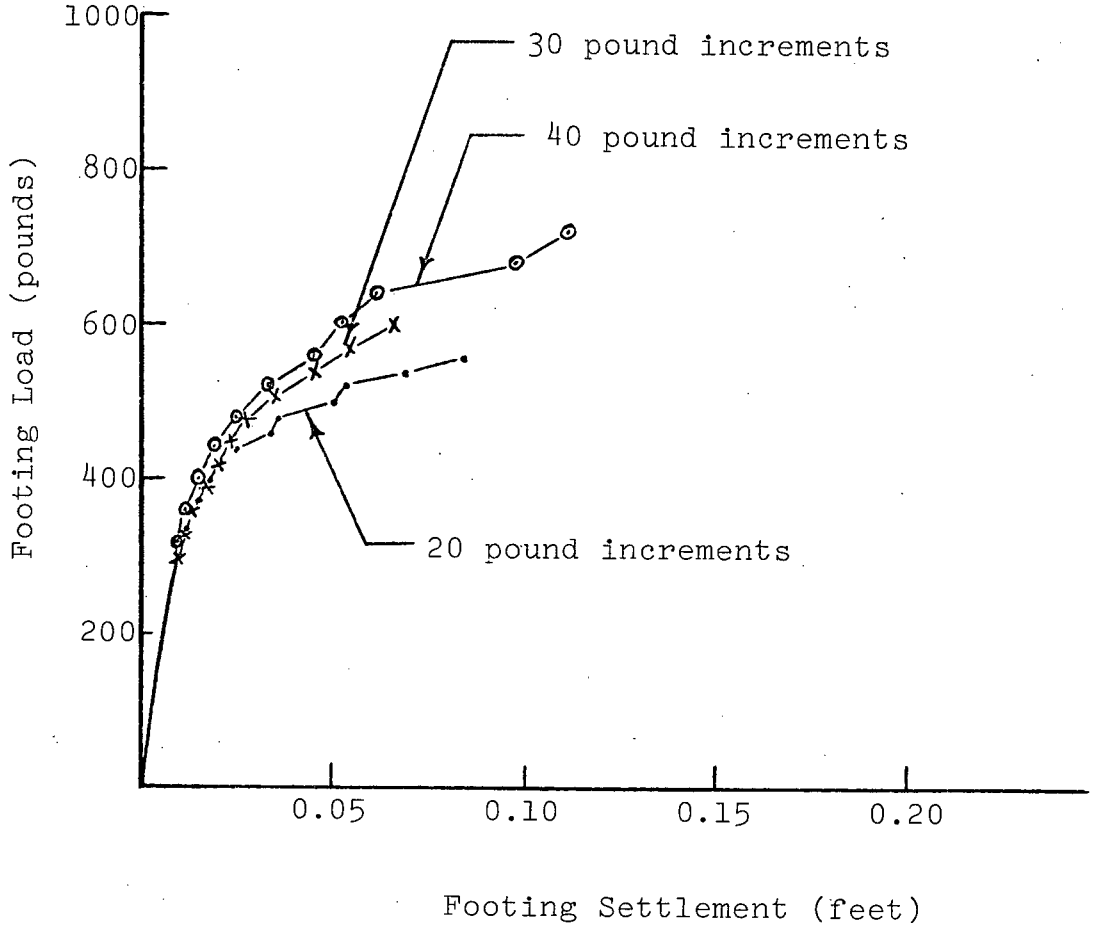

FIGURE 8 LOAD-SETTLEMENT CURVES FOR ANALYSES IN WHICH THE SHEAR MODULUS WAS REDUCED TO ONE-HUNDRED POUNDS PER SQUARE FOOT AT YIELD AND THE BULK MODULUS WAS NOT REDUCED AT YIELD

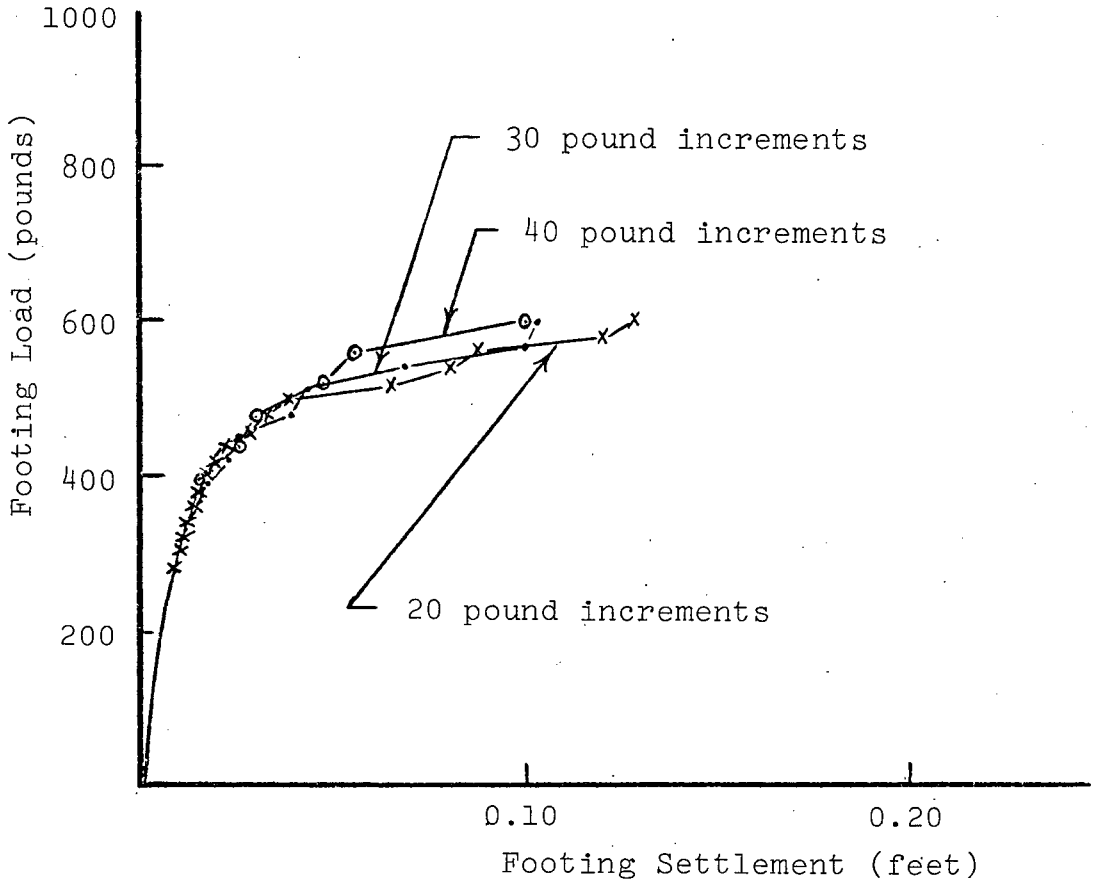

FIGURE 9 LOAD-SETTLEMENT CURVES FOR ANALYSES IN WHICH THE SHEAR MODULUS WAS REDUCED TO FIVE POUNDS PER SQUARE FOOT AT YIELD AND THE BULK MODULUS WAS NOT REDUCED AT YIELD

The predicted ultimate bearing capacity of the footing-soil system may be taken as the asymptote suggested by the predicted load-settlement curve. The asymptotes suggested by the load-settlement curves predicted in the analyses, in which the shear modulus of the sand was reduced to five pounds per square foot at yield, varied from about five-hundred and seventy pounds to about six-hundred and twenty pounds. The asymptotic load increased with increasing load increment size. The load-settlement curves predicted in the analyses, in which the shear modulus was reduced to one-hundred pounds per square foot at yield, did not flatten as much as those predicted in the analyses in which the shear modulus was reduced to five pounds per square foot at yield. The writer can only say that the asymptotes suggested by them were all greater than six hundred pounds. Again, the asymptotic load appeared to increase with increasing load increment size.

For comparison, the theoretical ultimate bearing capacity, assuming rigid-plastic behaviour of the footing-soil system, for the half of the six inch wide footing represented in the finite element mesh, as found with the Caquot-Kerisel bearing capacity factors given by Vesic (16), is five-hundred and thirty-seven pounds. This is six percent to fourteen percent lower than those predicted in the analyses in which the shear modulus was reduced to five pounds per square foot at yield and at least ten percent

lower than any of those predicted in the analyses in which the shear modulus was reduced to one-hundred pounds per square foot at yield.

The predicted load-settlement curves showed abrupt increases and decreases in their slopes after flattening out somewhat. These were due to elements which had previously failed coming out of failure, and, to elements which previously had not failed, failing with further increases in the load applied to the footing.

The locations of failed elements, predicted by the analysis in which the shear modulus was reduced to five pounds per square foot at yield and in which twenty pound load increments were used, are shown in Figure (10) for loads equal to and greater than that at which the load-settlement curve began to flatten out. The locations of failed elements do not suggest any clear failure mode.

The movements of nodes in the vicinity of the footing are shown in Figure (11) for the load increment from five-hundred and twenty pounds to five-hundred and forty pounds, in the analysis in which the shear modulus was reduced to five pounds per square foot at yield, and in which twenty pound load increments were used. The nodes appear to move in smooth trajectories beginning downward at the base of the footing and changing to horizontal and, finally, upward, away from the footing. This is similar to the motions reported by Vesic (16) for the general shear

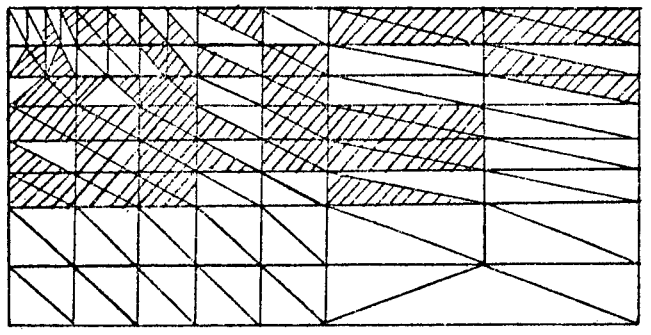

At 520 pounds

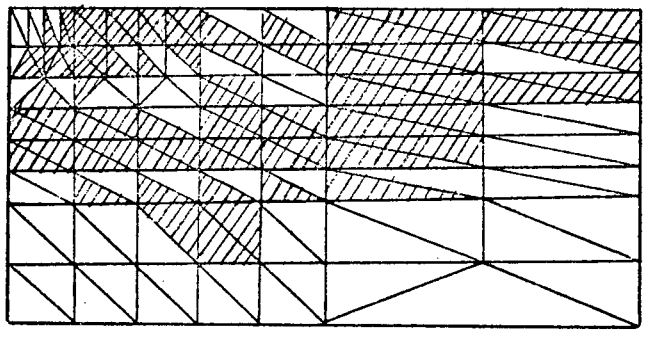

During Final Analysis of Increment from 520 pounds to 540 pounds

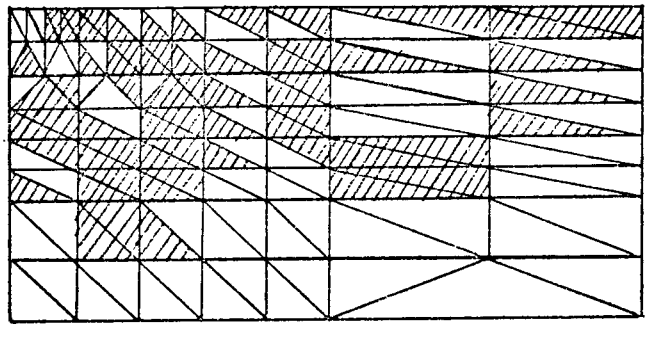

At 540 pounds

FIGURE 10 LOCATIONS OF FAILED ELEMENTS FOR THE ANALYSIS IN WHICH THE SHEAR MODULUS WAS REDUCED TO FIVE POUNDS PER SQUARE FOOT AT YIELD, THE BULK MODULUS WAS NOT REDUCED AT YIELD, AND TWENTY POUND LOAD INCREMENTS WERE USED

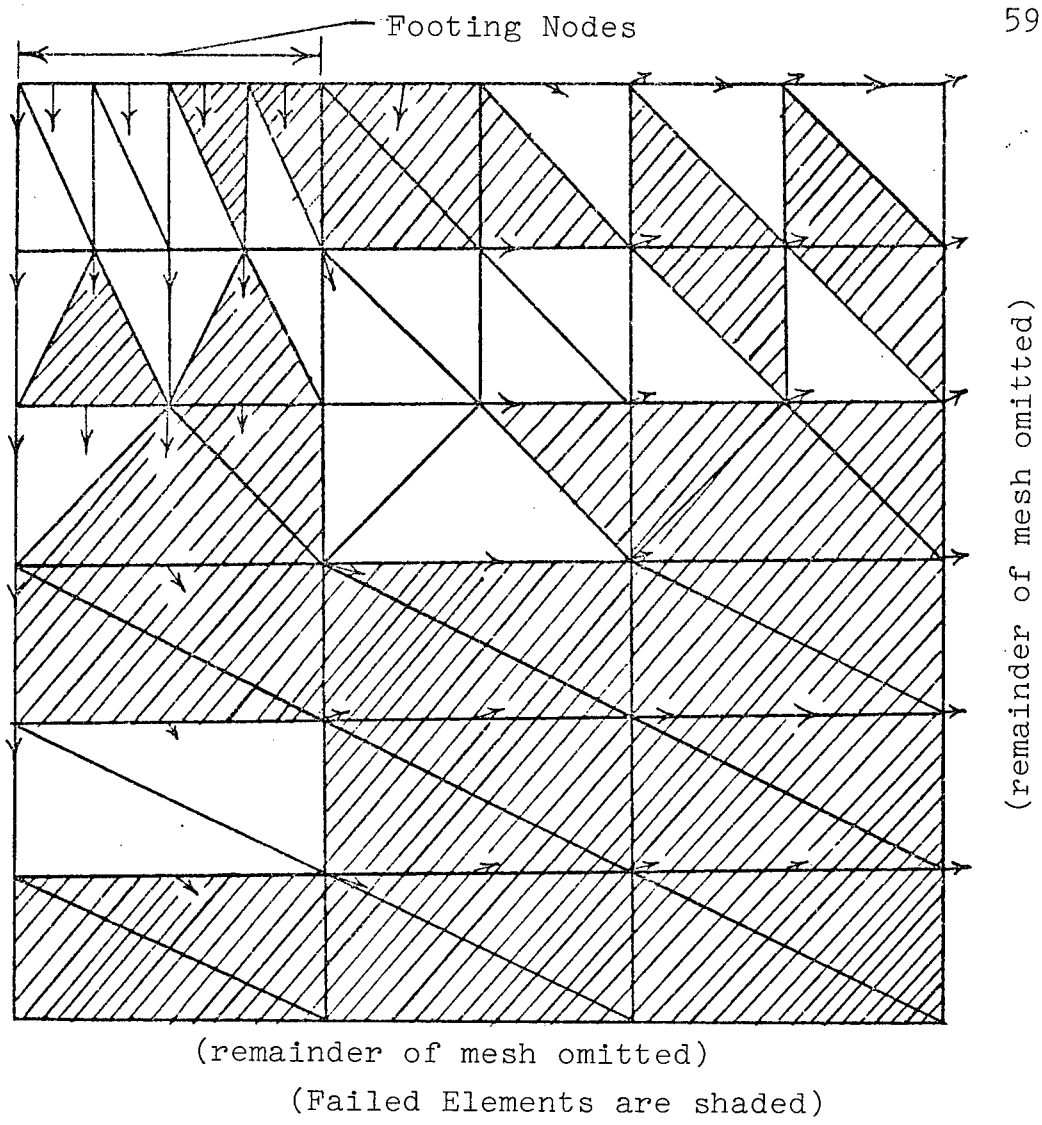

FIGURE 11 MOVEMENTS OF NODES DURING THE LOAD INCREMENT FROM FIVE HUNDRED AND TWENTY POUNDS TO FIVE HUNDRED AND FORTY POUNDS IN THE ANALYSIS IN WHICH THE SHEAR MODULUS WAS REDUCED TO FIVE POUNDS PER SQUARE FOOT AT YIELD, THE BULK MODULUS WAS NOT REDUCED AT YIELD, AND TWENTY POUND INCREMENTS WERE USED

failure of a strip footing on sand.

As was stated in section (3.4), it is common practice to use a constant value of Poisson's ratio throughout a nonlinear analysis of the load-deformation response of a soil body and simply to reduce the value of Young's modulus at yield. In order to assess the effect of this practice on the results of the analysis of the load-settlement response of the six inch wide surface strip footing, a second set of analyses was performed in which the value of Poisson's ratio for the sand was assumed to be 0.42 regardless of the state of stress, and the value of Young's modulus was reduced to one-hundred pounds per square foot at yield. The equation, used in this second set of analyses to relate the tangent value of Young's modulus to the state of stress prior to yield, was the same as that used in the first set of analyses. The finite element mesh used in the second set of analyses was the same as that used in the first set of analyses. The results of the second set of analyses are presented below.

The footing load-settlement curves predicted, using different size load increments in the analyses in which Poisson's ratio was assumed to have a constant value of 0.42 and in which Young's modulus was reduced to one hundred pounds per square foot at yield, are shown in Figure (12). The ultimate bearing capacity of the footing suggested by these load-settlement curves is less than about

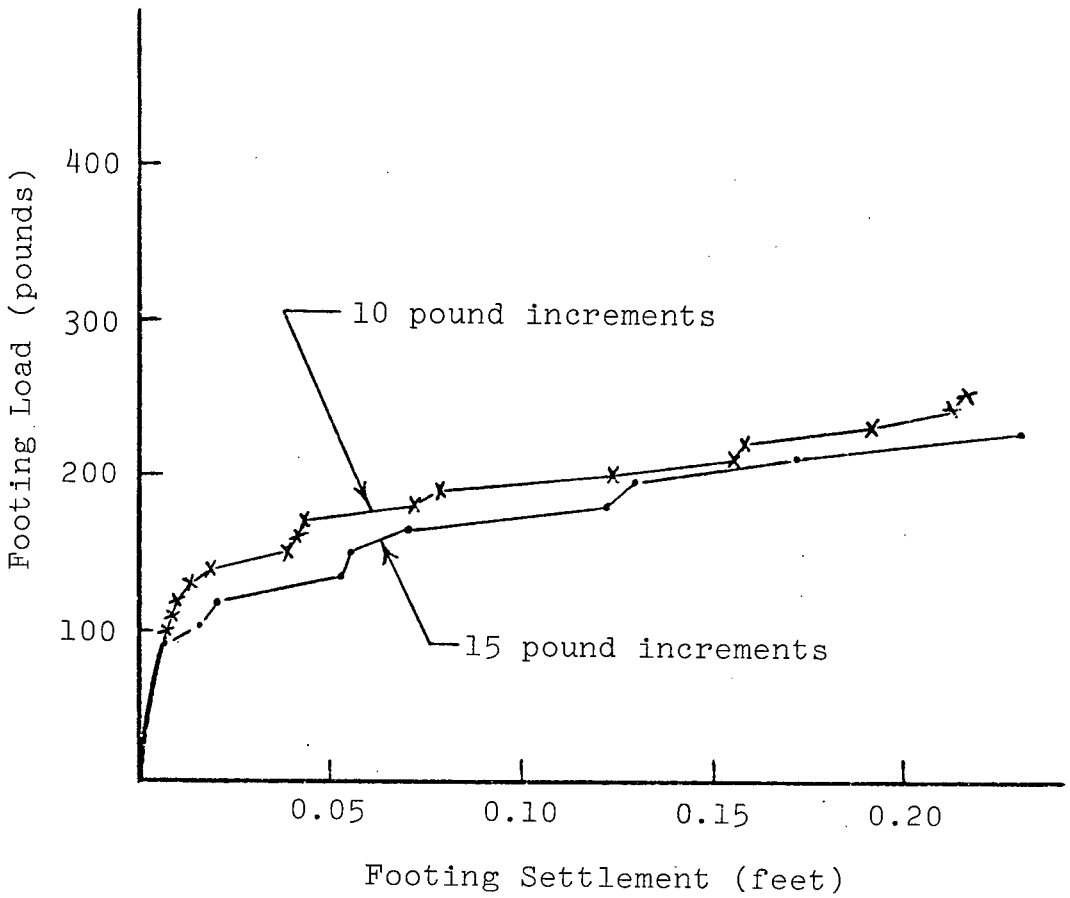

FIGURE 12 LOAD-SETTLEMENT CURVES FOR ANALYSES IN WHICH POISSON'S RATIO HAD A CONSTANT VALUE OF 0.42 AND YOUNG'S MODULUS WAS REDUCED TO ONE-HUNDRED POUNDS PER SQUARE FOOT AT YIELD

three hundred pounds. This is about one-half of that suggested by the load-settlement curves predicted in the first set of analyses, in which the shear modulus was reduced at yield while the bulk modulus was not.

The locations of failed elements, as predicted in the analysis in which Poisson's ratio had a constant value of 0.42 and Young's modulus was reduced to one-hundred pounds per square foot at yield and fifteen pound load increments were used, are shown in Figure (13) for loads equal to and greater than that at which the load-settlement curve began to flatten out. The locations of failed elements do not suggest any clear failure mode.

The movements of nodes in the vicinity of the footing are shown in Figure (14) for the load increment from one-hundred and twenty pounds to one-hundred and thirty-five pounds in the analysis in which Poisson's ratio had a constant value of 0.42, Young's modulus was reduced to one hundred pounds per square foot at yield, and fifteen pound load increments were used. From this figure, it is apparent that the footing failed by compression of the failed elements directly beneath it. The only significant motions were vertical motions of the nodes directly beneath the footing. This behaviour is very different from that predicted in the analyses in which the shear modulus was reduced at yield while the bulk modulus was not.

The difference between the load-deformation

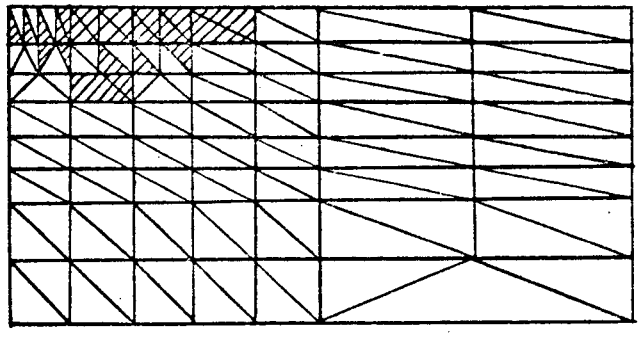

At 120 pounds

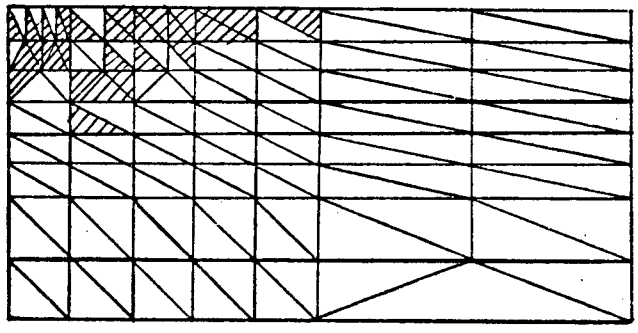

During Final Analysis of Increment from 120 pounds to 135 pounds

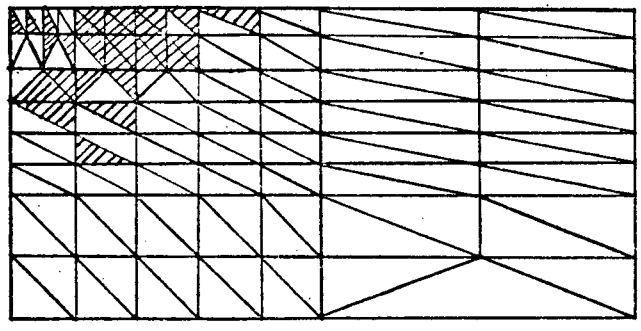

At 135 pounds

FIGURE 13 LOCATIONS OF FAILED ELEMENTS FOR THE ANALYSIS IN WHICH POISSON'S RATIO HAD A CONSTANT VALUE OF 0.42, YOUNG'S MODULUS WAS REDUCED TO FIVE POUNDS PER SQUARE FOOT AT YIELD, AND FIFTEEN POUND LOAD INCREMENTS WERE USED

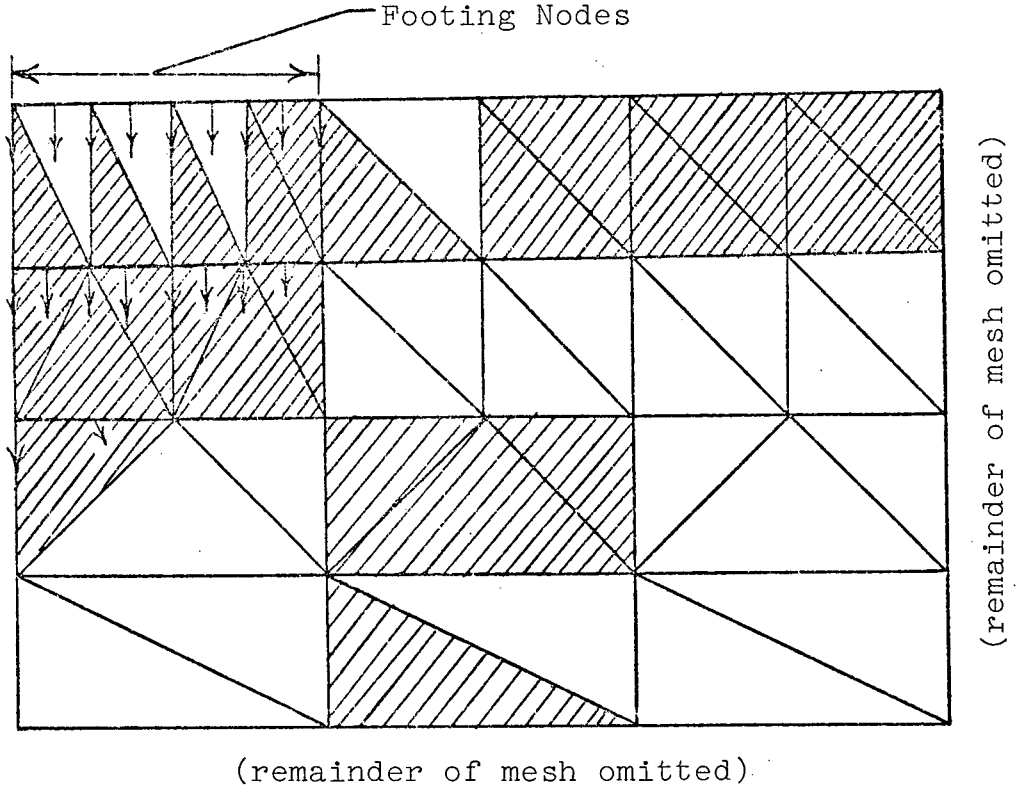

FIGURE 14 MOVEMENTS OF NODES DURING THE LOAD INCREMENT FROM ONE-HUNDRED AND TWENTY POUNDS TO ONE-HUNDRED AND THIRTY-FIVE POUNDS IN THE ANALYSIS IN WHICH POISSON'S RATIO HAD A CONSTANT VALUE OF 0.42, YOUNG'S MODULUS WAS REDUCED TO ONE-HUNDRED POUNDS PER SQUARE FOOT AT YIELD, AND FIFTEEN POUND LOAD INCREMENTS WERE USED

response of the footing-soil system predicted in the first set of analyses and that predicted in the second set of analyses resulted from the difference between the way in which yield of the sand was taken into account in each analysis. In the first set of analyses, the shear modulus was reduced at yield but the bulk modulus was the same after yield as it was immediately prior to yield. This practice reduces the resistance of the elements to shear deformations at yield but does not reduce their resistance to normal deformations. Therefore, in the first set of analyses, the yielded elements beneath the footing could not be easily compressed by further increases in the load applied to them. In the second set of analyses, the value of Poisson's ratio was constant but the value of Young's modulus was reduced at yield of the sand. This practice reduces the values of both the shear and the bulk moduli at yield. Therefore, in the second set of analyses, the resistance of elements to both shear and normal deformations was reduced at yield. This allowed the yielded elements directly beneath the footing to be compressed easily by further increases in the load applied to them.

Since the resistance of a real sand to normal strains is not significantly reduced at yield, as defined by the Mohr-Coulomb failure criterion, the behaviour of the footing-soil system predicted in the first set of analyses is more realistic than that predicted in the second set of analyses.

CHAPTER 5

CONCLUSION

Existing methods of predicting the nonlinear load-deformation response of soils and soil structures are based on incremental iterative elastic analysis. A solution for a load increment is considered acceptable if the stresses and strains computed for the end of the load increment conform to the stress-strain relations of the material within a prescribed tolerance. Convergence to the stress-strain relations of the material may be achieved in two ways: first, the computed strains may be considered correct and the computed stresses successively corrected to make them conform to the stress-strain relations of the material; and secondly, the computed stresses may be assumed to be correct and the strains successively corrected to make them compatible with the stress-strain relations of the material and the computed stresses. The first objective is accomplished by iterative adjustment of the elastic properties used in the analysis of the response to the load increment; the second by a Newton-Raphson approach in which the elastic properties are not changed.

Methods of incremental analysis in which both the computed stresses and computed strains are made to conform to the stress-strain relations of the material by

iterative adjustment of the elastic properties have the advantage of simplicity. However, they require a considerable computational effort since the stiffness matrix of the soil body must be rebuilt prior to each successive adjustment. For this reason, it is common practice to perform only one iteration per load increment and not to use a convergence criterion. Also, since one iterates on the elastic properties used, the accuracy with which the computed stresses and strains conform to the stress-strain relations of the material is not directly controlled.

The modified Newton-Raphson method has the advantage that the stiffness matrix of the body under consideration is not rebuilt during the iterative correction of the computed strains. This saves considerable computational effort.

The modified Newton-Raphson method is readily applied to problems in which a single known stress-strain curve is followed. However, in problems involving soils, a family of stress-strain curves is usually used and the stress-strain curve followed by a point within the soil mass changes with the state of stress at that point if the stress-path followed is not that for which the curves were obtained. As was explained in section (4.1.2), this makes the application of the modified Newton-Raphson method to problems involving soils more difficult.

The accuracy with which the load-deformation

response of soils and soil structures can be predicted is limited mainly by the accuracy with which the stress-strain properties of the soil are represented. The stress-strain relations currently used are based on the assumption that soils are isotropic elastic materials and have two major sources of error: the effect of stress-path is neglected; and the anisotropy of soils is neglected.

Ideally, one should use stress-strain relations which take the stress-path dependent behaviour and anisotropy of soils into account. While this is possible, the development of such stress-strain relations would require the evaluation of more stress-strain properties and considerably more effort than does the development of those currently used.

Although the behaviour of soils after yield is generally that of a plastic material, many authors deal with soils after yield as soft elastic materials. They simply reduce the values of the elastic moduli at yield. For a real soil, the resistance to shear stresses is reduced at yield whereas the resistance to normal stresses is not. Therefore, while the shear modulus is reduced at yield, the bulk modulus is not.

If one deals with soils as soft elastic materials after yield one must be careful that the value of the bulk modulus is not reduced at yield. The practice of using a constant value of Poisson's ratio and reducing the value

of Young's modulus at yield is unacceptable since it results in a reduction of the values of both the shear modulus and the bulk modulus. Analyses of the response of a strip footing on sand to vertical loading, performed by the writer, show that this leads to unrealistic behaviour in yielded soil elements. The yielded elements were too compressible. This affected to a great extent both the modes of failure of the footing-soil system and failure loads predicted in the analyses.

Nonlinear analyses of the load-deformation response of soils and soil structures should be performed using the shear modulus and bulk modulus to define the soil's stress-strain relations. At yield, the value of the shear modulus should be reduced and the bulk modulus left unchanged. As far as possible, the elastic moduli and stress-strain relations used should model the effect of stress-path on the soil stress-strain properties.

BIBLIOGRAPHY

1. Brebbia, C.A. and Connor, J.J., Fundamentals of Finite Element Techniques, Halstead Press, John Wiley and Sons Ltd., New York-Toronto, 1974, pp. 129-138.

2. Corotis, R.B., Farzin, M.H. and Krizek, R.J., "Nonlinear Stress-Strain Formulation for Soils," Journal of the Geotechnical Engineering Division, ASCE, Vol. 100, No. GT9, September, 1974, pp. 993-1008.

3. Deming, W.E., Statistical Adjustment of Data, Dover Publications Inc., New York, New York, 1943.

4. Desai, C.S. and Abel, J.F., Introduction to the Finite Element Method, Van Nostrand Reinhold Co., New York, New York, 1972.

5. Domaschuk, L. and Valliappan, P., "Nonlinear Settlement Analysis by Finite Element," Journal of the Geotechnical Engineering Division, ASCE, Vol. 101, No. GT7, July, 1975, pp. 601-614.

6. Domaschuk, L. and Wade, N.H., "A Study of Bulk and Shear Moduli of a Sand," Journal of the Soil Mechanics and Foundations Division, ASCE, Vol. 95, No. SM2, March, 1969, pp. 561-581.

7. Drnevich, V.P., "Constrained and Shear Moduli for Finite Elements," Journal of the Geotechnical Engineering Division, ASCE, Vol. 101, No. GT5, May, 1975, pp. 459-473.

8. Duncan, J.M., "Static Finite Element Analysis," notes for extension course entitled Recent Developments in the Design, Construction and Performance of Embankment Dams, College of Engineering, University of California, Berkeley, California, June, 1975.

9. Duncan, J.M. and Chang, C.Y., "Nonlinear Analysis of Stress and Strain in Soils," Journal of the Soil Mechanics and Foundations Division, ASCE, Vol. 96, No. SM5, September, 1970, pp. 1629-1653.

10. Duncan, J.M. and Chang, C.Y., "Nonlinear Analysis of Stress and Strain in Soils-Closure," Journal of the Soil Mechanics and Foundations Division, ASCE, Vol. 98, No. SM5, May, 1972, pp. 495-498.

11. Finn, W.D.L. and Miller, R.I.S., "Nonlinear Analysis of Earth Structures," Numerical Methods in Geomechanics, ed. C.S. Desai, ASCE, New York, New York, 1976, pp. 195-204.

12. Girijavallabhan, C.V. and Reese, L.C., "Finite Element Method for Problems in Soil Mechanics," Journal of the Soil Mechanics and Foundations Division, ASCE, Vol. 94, No. SM2, March, 1968, pp. 473-496.

13. Lade, P.V. and Duncan, J.M., "Stress-Path Dependant Behaviour of Cohesionless Soil," Journal of the Geotechnical Engineering Division, ASCE, Vol. 102, No. GT1, January, 1976, pp. 51-68.

14. Nyak, G.C. and Zienkiewicz, O.C., "Elasto-Plastic Stress Analysis. A Generalization for Various Constitutive Relations Including Strain Softening," International Journal for Numerical Methods in Engineering, Vol. 5, No. 1, September-October, 1972, pp. 113-135.

15. Roy, J., 'Nonlinear Analysis of the Undrained Shear Strength of Clay,' a research project submitted in partial fulfillment of the requirement for the degree of Master of Engineering, Dept. of Civil Engineering, University of British Columbia, 1974, unpublished.

16. Vesic, A.S., "Analysis of Ultimate Loads of Shallow Foundations," Journal of the Soil Mechanics and Foundations Division, ASCE, Vol. 99, No. SM1, January, 1973, pp. 45-73.

17. Wong, K.S. and Duncan, J.M., 'Hyperbolic Stress-Strain Parameters for Nonlinear Finite Element Analyses of Stresses and Movements in Soil Masses,' Report No. TE-74-3 to National Science Foundation, Dept. of Civil Engineering, Institute of Transportation and Traffic Engineering, University of California, Berkeley, California, 1974.

18. Yudhbir and Varadarajan, A., "Stress-Path Dependent Deformation Moduli of Clay," Journal of the Geotechnical Engineering Division, ASCE, Vol. 101, No. GT3, March, 1975, pp. 315-327.

19. Zienkiewicz, O.C., 'The Finite Element Method in Engineering Science,' McGraw-Hill Book Co., Ltd., London, England, 1971, pp. 369-377.

APPENDIX 1

DERIVATION OF THE STIFFNESS MATRIX FOR THE LINEAR STRAIN TRIANGULAR ELEMENT

The element stiffness matrix which relates the nodal forces, {Q}, and the nodal displacements, {q}, for the linear strain triangular element shown in Figure 15 may be derived as follows:

The displacements, {u}, of a point, p, within the linear strain triangular element are related to the nodal displacements, {q}, by the equation

$$\{u\} = \begin{Bmatrix} u_x \\ u_y \end{Bmatrix} = [A]\{q\} \qquad (1)$$

where [A] as given by Desai and Abel (4), in terms of natural coordinates, is

$$[A] \doteq \begin{bmatrix} \zeta_1(2\zeta_1 - 1) & 0 \\ 0 & \zeta_1(2\zeta_1 - 1) \\ \zeta_2(2\zeta_2 - 1) & 0 \\ 0 & \zeta_2(2\zeta_2 - 1) \\ \zeta_3(2\zeta_3 - 1) & 0 \\ 0 & \zeta_3(2\zeta_3 - 1) \\ 4\,\zeta_1\zeta_2 & 0 \\ 0 & 4\,\zeta_1\zeta_2 \\ 4\,\zeta_2\zeta_3 & 0 \\ 0 & 4\,\zeta_2\zeta_3 \\ 4\,\zeta_3\zeta_1 & 0 \\ 0 & 4\,\zeta_3\zeta_1 \end{bmatrix} \qquad (2)$$

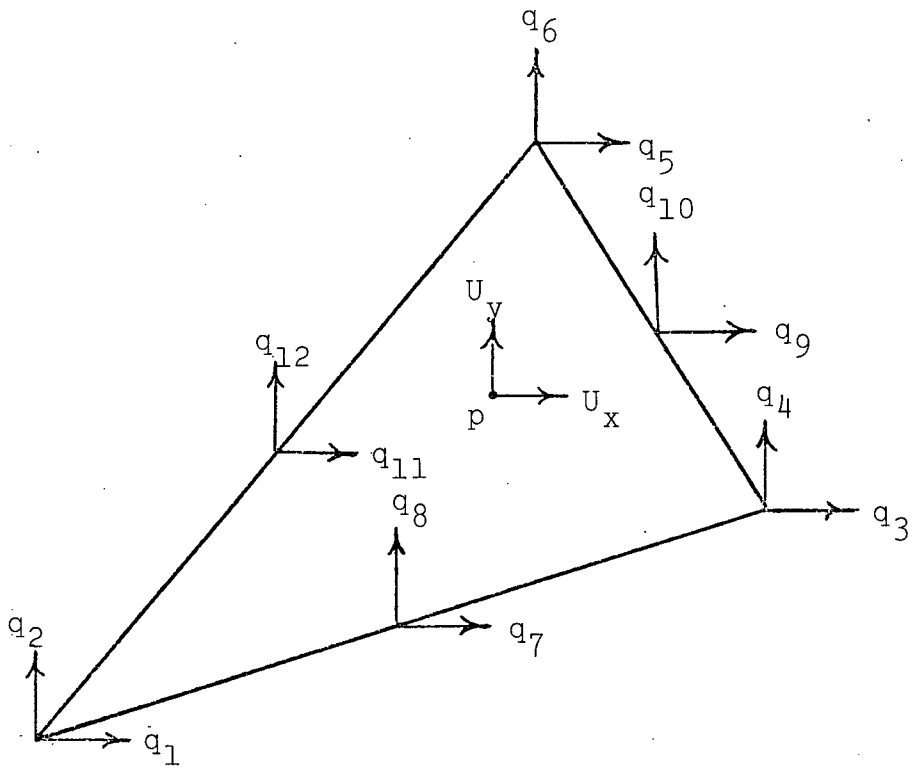

FIGURE 15 LINEAR STRAIN TRIANGULAR ELEMENT

in which

$$\zeta_1 = \frac{A_1}{A} \qquad \zeta_2 = \frac{A_2}{A} \quad \text{and} \quad \zeta_3 = \frac{A_3}{A}$$

where A is the area of the triangular element and A_i is the area of the point p and the nodes opposite node i as illustrated in Figure 16.

The relationship between the strains, $\{\varepsilon\}$, at any point within the element and the nodal displacements, $\{q\}$, for plane strain is

$$\{\varepsilon\} = \begin{Bmatrix} \varepsilon_x \\ \varepsilon_y \\ \gamma_{xy} \end{Bmatrix} = [L]\,[A]\,\{q\} = [B]\,\{q\} \qquad (3)$$

in which

$$L = \begin{bmatrix} \delta/\delta_x & 0 \\ 0 & \delta/\delta_y \\ \delta/\delta_y & \delta/\delta_x \end{bmatrix} \qquad (4)$$

For natural coordinates, Desai and Abel (4) give the following differentiation formulae:

$$\frac{\delta U_x}{\delta X} = \frac{b_m}{2A}\,\frac{\delta U_x}{\delta \zeta_m} \qquad (5)$$

in indicial notation where

$$b_1 = y_2 - y_3$$
$$b_2 = y_3 - y_1$$
$$b_3 = y_1 - y_2$$

and

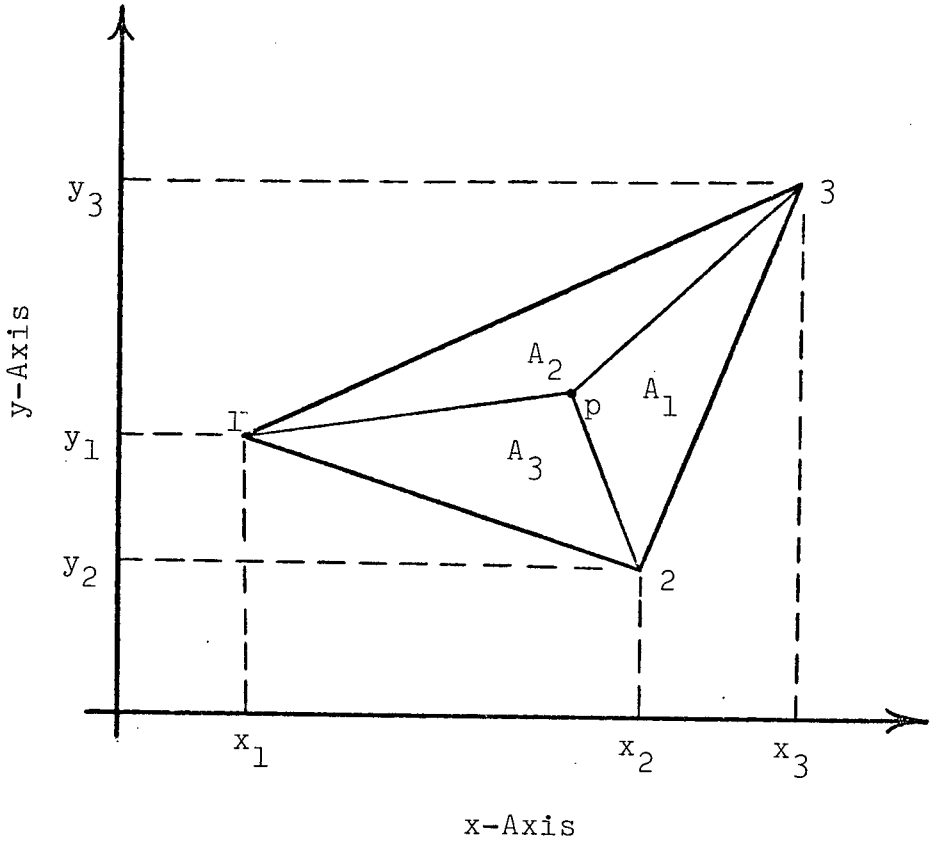

FIGURE 16 AREAS FOR NATURAL COORDINATES

$$\frac{\delta U_x}{\delta y} = \frac{a_m}{2A} \frac{\delta U_x}{\delta \zeta_m} \tag{6}$$

in indicial notation where

$$a_1 = x_2 y_3 - x_3 y_2$$

$$a_2 = x_3 y_1 - x_1 y_3$$

$$a_3 = x_1 y_3 - x_2 y_1$$

and similar formulae for the other derivatives.

The matrix [B] in equation (3) is then

$$[B] = \frac{2}{A} \begin{bmatrix} (\zeta_1 - \frac{1}{4})b_1 & 0 & (\zeta_1 - \frac{1}{4})a_1 \\ 0 & (\zeta_1 - \frac{1}{4})a_1 & (\zeta_1 - \frac{1}{4})b_1 \\ (\zeta_2 - \frac{1}{4})b_2 & 0 & (\zeta_2 - \frac{1}{4})a_2 \\ 0 & (\zeta_2 - \frac{1}{4})a_2 & (\zeta_2 - \frac{1}{4})b_2 \\ (\zeta_3 - \frac{1}{4})b_3 & 0 & (\zeta_3 - \frac{1}{4})a_3 \\ 0 & (\zeta_3 - \frac{1}{4})a_3 & (\zeta_3 - \frac{1}{4})b_3 \\ \zeta_2 b_1 + \zeta_1 b_2 & 0 & \zeta_2 a_1 + \zeta_1 a_2 \\ 0 & \zeta_2 a_1 + \zeta_1 a_2 & \zeta_2 b_1 + \zeta_1 b_2 \\ \zeta_3 b_2 + \zeta_2 b_3 & 0 & \zeta_3 a_2 + \zeta\ a_3 \\ 0 & \zeta_3 a_2 + \zeta_2 a_3 & \zeta_3 b_2 + \zeta_2 b_3 \\ \zeta_1 b_3 + \zeta_3 b_1 & 0 & \zeta_1 a_3 + \zeta_3 a_1 \\ 0 & \zeta_1 a_3 + \zeta_3 a_1 & \zeta_1 b_3 + \zeta_3 b_1 \end{bmatrix} \tag{7}$$

The stresses, $\{\sigma\}$, at any point in a linear elastic material are related to the strains, $\{\varepsilon\}$, at that point by the equation

$$\{\sigma\} = \begin{Bmatrix} \sigma_x \\ \sigma_y \\ \tau_{xy} \end{Bmatrix} = [D]\{\varepsilon\} \tag{8}$$

for plane strain conditions. For an isotropic elastic material

$$[D] = \begin{bmatrix} k + \frac{4}{3}G & k - \frac{2}{3}G & 0 \\ k - \frac{2}{3}G & k + \frac{4}{3}G & 0 \\ 0 & 0 & G \end{bmatrix} \tag{9}$$

in which k is the bulk modulus and G is the shear modulus.

For equilibrium, by the principal of virtual work, the work done by the real external loads, $\{Q\}$, acting through the virtual nodal displacements, $\{\bar{q}\}$, must be equal to the work done by the real internal stresses, $\{\sigma\}$, acting through the virtual strains, $\{\bar{\varepsilon}\}$, corresponding to the virtual nodal displacements. Therefore,

$$\int_V \{\bar{\varepsilon}\}^T \{\sigma\}\, dV = \{q\}^T \{Q\} \tag{10}$$

which, upon the introduction of equations (3) and (8) becomes

$$\int_V \{\bar{q}\}^T [A]^T [L]^T [D][L][A]\{q\} dV = \{\bar{q}\}^T \{Q\} \tag{11}$$

and since $\{\bar{q}\}^T$ and $\{q\}$ are not functions of position,

$$\left[\int_V [A]^T[L]^T[D][L][A]dV \right] = \{Q\} \qquad (12)$$

or $[K]\{q\} = \{Q\}$

where [K] is called the element stiffness matrix.

APPENDIX 2

STRESS-STRAIN SUBROUTINES

The writer developed stress-strain subroutines based on earlier work done by Roy (15) to allow the use of the hyperbolic stress-strain relations of Duncan and Chang (9) with the finite element program NONLIN. These subroutines control the iterative process and use equations (3-18) and (3-19) to relate the tangent values of Young's modulus and Poisson's ratio to the state of stress at the element centroids. The iterative process used is the one iteration per load increment method described in section (2.2.1). The subroutines were written in FORTRAN and are presented below. All FORTRAN variables and arrays are defined where they appear. The functions of the subroutines are explained at the start of each subroutine.

```
      SUBROUTINE SETUP(X)
C
C     THIS SUBROUTINE, TOGETHER WITH SUBROUTINE EU, CALCULATES
C     THE INITIAL BULK AND SHEAR MODULI FOR THE ELEMENTS.
C
      IMPLICIT REAL*8(A-H,O-Z)
      DIMENSION X(50)
      COMMON /CNSTIT/PATRN(10,10),NCONST,IPLANE
      COMMON/EUBLK/ISTEP,NSTEP,KSTEP,IFGA
      DATA ISTRT/0/
C
      NSTEP=0
      KSTEP=1
      IFGA=0
      IF(ISTRT.EQ.0) ISTEP=0
      ISTRT=1
C
C     THE ARRAY X CONTAINS THE FOLLOWING ELEMENT INFORMATION:
C
C     1     SOIL UNIT WEIGHT
C     2     COHESION INTERCEPT, C
C     3     ANGLE OF INTERNAL FRICTION IN DEGREES
C     4     FAILURE RATIO, RF
C     5     MODULUS NUMBER, K
C     6     MODULUS EXPONENT, N
C     7     MODULUS AFTER FAILURE
C     8     POISSON'S RATIO PARAMETER,G
C     9     THICKNESS(PLANE PROBLEMS ONLY)
C     10-15 INITIAL ELEMENT STRESSES:SIGX,SIGY,SIGZ,TAUXY,TAUYZ,TAUZX
C     16    INITIAL ELEMENT PORE PRESSURE
C     17-22 ZERO STRAINS EPSX,EPSY,EPSZ,GAMXY,GAMYZ,GAMZX
C     34    POISSON'S RATIO PARAMETER,F
C     35    POISSON'S RATIO PARAMETER,D
C     36    TENSILE STRENGTH
C     37    ATMOSPHERIC PRESSURE, PATM
```

```
C       38    SCRATCH SPACE (NOT USED)
C       39    SCRATCH SPACE (NOT USED)
C       40    COEFFICIENT OF LATERAL EARTH PRESSURE, KO
C
C       ON RETURN, X CONTAINS THE ADDITIONAL INFORMATION BELOW.
C
C       23    INITIAL YIELD FUNCTION
C       24    INITIAL BULK MODULUS
C       25    INITIAL SHEAR MODULUS
C
        X(23)=0.D0
C
C       CALCULATE THE INITIAL BULK AND SHEAR MODULI.
C
        CALL EU(ET,UT,X(10),X(2),X(34))
C
C       COMPUTE THE INITIAL BULK AND SHEAR MODULI
C
        X(24)=UT
        X(25)=ET/(3.D0-(ET/(3.D0*UT)))
C
C       X(24) AND X(25) CONTAIN THE INITIAL BULK AND SHEAR MODULI.
C
        RETURN
        END
C
        SUBROUTINE STIFLT(X,SSS,DEPS1,EPSV,EPSA)
C
C       THIS SUBROUTINE, TOGETHER WITH SUBROUTINES EU AND EUD,
C       CONTROLS THE STRESS-STRAIN BEHAVIOUR OF THE FINITE ELEMENTS.
C
C  ARRAY X CONTAINS:
C       1     SOIL UNIT WEIGHT
C       2     COHESION INTERCEPT, C
C       3     ANGLE OF INTERNAL FRICTION IN DEGREES
C       4     FAILURE RATIO, RF
```

```
C      5     MODULUS NUMBER, K
C      6     MODULUS EXPONENT, N
C      7     MODULUS AFTER FAILURE
C      8     POISSON'S RATIO PARAMETER,G
C      9     THICKNESS(PLANE PROBLEMS ONLY)
C      10-15 STRESSES AT THE END OF LAST STEP (UPDATED BY STIFLT)
C      16    PORE PRESSURE AT THE END OF LAST STEP(UPDATED BY STIFLT)
C      17-22 ZERO STRAINS EPSX,EPSY,EPSZ,GAMXY,GAMYZ,GAMZX
C      23    YIELD FUNCTION
C      24-33 MODULI USED IN PREVIOUS STEP. RETURNED MODULI FOR NEXT STEP.
C      34    POISSON'S RATIO PARAMETER,F
C      35    POISSON'S RATIO PARAMETER,D
C      36    SCRATCH SPACE (NOT USED)
C      37    ATMOSPHERIC PRESSURE, PATM
C      38    SCRATCH SPACE (NOT USED)
C      39    SCRATCH SPACE (NOT USED)
C      40    COEFFICIENT, KO
C      X(41)-X(50) MAY BE INITIALIZED FOR SUBSEQUENT USE IN STIFLT.
C      SSS IS TO RETURN THE MODULI WHICH ARE TO BE USED WHEN
C      THE STEP IS REITERATED.
C      DEPS IS THE INCREMENTAL STRAINS FOR THE LAST STEP.
C      EPSV IS THE STRAIN VELOCITIES AT THE PRESENT TIME.
C      EPSA IS THE STRAIN ACCELERATIONS AT THE PRESENT TIME.
C
       IMPLICIT REAL*8(A-H,O-Z)
       REAL*8 X(63),SSS(10),DEPS(6),EPSV(6),EPSA(6),D(16),SD(4),DEPS1(6)
       INTEGER*2 IFAL(500),IADO
       COMMON /FALBLK/DT,DELTAT,DTNEXT,IRESTP,IELT,IFGO,ICHNG,IFAL,
      * IPLANE,IDEBUG,ISTAT,IFDT,IFDIAG,ITMAX,LSTEP,IFERRF
       COMMON/EUBLK/ISTEP,NSTEP,KSTEP,IFGA
C
       NSTEP=1
       IFGA=IFGO
C
C  /FALBLK/ CONTAINS GOVERNING INFORMATION FOR THE PROGRAM AS A WHOLE.
C
```

```
C  IRESTP  IS THE ITERATION NUMBER (1 ON THE FIRST PASS).
C  IELT    IS THE NUMBER OF THE ELEMENT BEING PROCESSED BY STIFLT.
C  IFGO    IS A FLAG SET WHEN THE ACCURACY CRITERION IS VIOLATED
C          FOR A GIVEN STEP. IF NOT 0 IT CAUSES THE STEP TO BE
C          REPEATED (UNLESS IRESTP>ITMAX).
C  ICHNG   IS A FLAG TO INDICATE THAT THE ELEMENT MODULI FOR
C          THE NEXT STEP ARE THE SAME AS FOR THE PREVIOUS STEP.
C
C  OF THESE, ONLY IFGO AND ICHNG ARE CHANGED BY STIFLT
C
C
C     UPDATE THE ELEMENT STRESSES.
C
      IF(IRESTP.GT.1) GO TO 100
      IFGO=1
      DO 101 I=1,4
  101 DEPS(I)=DEPS1(I)/2.D0
   99 CALL GETD(X(24),D)
      CALL BLOWUP(D,D,4)
      CALL DGMATV(D,DEPS,SD,4,4,4)
      DO 1 I=1,4
    1 X(I+9)=X(I+9)+SD(I)
C
C     CALCULATE NEW MODULI.
C     IF ELEMENT HAS YIELDED, THE BULK MODULUS IS
C     NOT CHANGED FROM ITS LAST VALUE.
C
      CALL EU(ET,UT,X(10),X(2),X(34))
C
      IF(UT.EQ.0.0D0) GOTO 500
      X(24)=UT
      X(25)=ET/(3.D0-(ET/(3.D0*UT)))
      GOTO 600
  500 CONTINUE
      X(25)=ET
  600 CONTINUE
```

```
C
C       X(24) AND X(25) ARE THE BULK AND SHEAR MODULI RESPECTIVELY.
C
        SSS(1)=X(24)
        SSS(2)=X(25)
        ICHNG=1
C
        RETURN
C
  100   IFGO=0
        DO 102 I=1,4
  102   DEPS(I)=DEPS1(I)
        GO TO 99
C
        END
C
        SUBROUTINE EUD(ET,UT,STRESS,PROP1,PROP2,CR,S1,S3,ISTEP,NEB)
C
C       THIS SUBROUTINE CHECK FOR FAILURE AND COMPUTES THE
C       VALUES OF YOUNG'S MODULUS AND POISSON'S RATIO.
C       (REF: DUNCAN AND CHANG, ASCE,JOUR. OF S.M.&F.E. DIV.,VOL.96,
C       NO.SM5, SEPTEMBER,1970)
C
        IMPLICIT REAL*8(A-H,O-Z)
        DIMENSION STRESS(14),PROP1(7),PROP2(7)
C
        IF(NEB.GT.1)WRITE(6,60) CR,S1,S3
   60   FORMAT('CR=',F10.5,'S1=',F10.5,'S3=',F10.5)
        FA=PROP1(2)/57.28D0
        CO=DCOS(FA)
        SI=DSIN(FA)
        FFF=2.D0*PROP1(1)*CO+(S1+S3)*SI
        IF(NEB.GT.1) WRITE(6,90) FFF
   90   FORMAT('FFF=',F10.5)
        RCS=2.D0*(PROP1(1)*CO +S3*SI)/(1.D0-SI)
        HCS=RCS/PROP1(3)
```

```
      S3OPA=S3/PROP2(4)
      FS=2.D0*CR/FFF
      STRESS(14)=FS
C
C     TEST FOR FAILURE USING MOHR-COULOMB CRITERION.
C
      IF(FS.LT.1.D0) GOTO 31
      WRITE(6,70) ISTEP
   70 FORMAT('ELEMENT',I5,'HAS FAILED BY MOHR-COULOMB')
C
C     TEST FOR TENSILE FAILURE.
C
   31 IF(S3.GT.0.D0)GOTO 33
      WRITE(6,41) ISTEP
   41 FORMAT('TENSILE FAILURE IN ELEMENT',I5)
      GOTO 30
C
C     CALCULATE TANGENT MODULUS FOR UNFAILED ELEMENT.
C
   33 IF(FS.GE.1.D0)GOTO 30
      EI=PROP1(4)*PROP2(4)*(S3OPA**PROP1(5))
      ET=EI*((1.D0-(2.D0*CR/HCS))**2)
      IF(ET.LT.PROP1(6)) ET=PROP1(6)
      GO TO 40
C
C     CALCULATE MODULUS AND POISSON'S RATIO FOR FAILED ELEMENT.
C
   30 ET=PROP1(6)
      UT=0.0D0
      GO TO 50
C
C     COMPUTE POISSON'S RATIO FOR UNFAILED ELEMENT.
C
   40 STRAIN=2.D0*CR/(EI*(1.D0-(2.D0*CR/HCS)))
      PRAT=PROP1(7)-PROP2(1)*DLOG10(S3OPA)
      UT=PRAT/(1.D0-PROP2(2)*STRAIN)**2
```

```
   50 IF(UT.GT.0.495D0) UT=0.495D0
C
C     ET= YOUNG'S MODULUS AND UT= POISSON'S RATIO.
C
      RETURN
      END
C
      SUBROUTINE EU(ET,UT,STRESS,PROP1,PROP2)
C
C
C     THIS SUBROUTINE, TOGETHER WITH EUD, COMPUTES THE
C     APPROPRIATE MODULI FOR THE FINITE ELEMENTS.
C
C     PROP1(1)=COHESION,C
C     PROP1(2)=THE ANGLE OF INTERNAL FRICTION
C     PROP1(3)=THE FAILURE RATIO, RF
C     PROP1(4)=THE MODULUS NUMBER, K
C     PROP1(5)=THE MODULUS EXPONENT, N
C     PROP1(6)=MODULUS AFTER FAILURE
C     PROP1(7)=POISSON'S RATIO PARAMETER, G
C     PROP2(1)=POISSON'S RATIO  PARAMETER, F
C     PROP2(2)=POISSON'S RATIO PARAMETER, D
C     PROP2(3)=SCRATCH SPACE (NOT USED)
C     PROP2(4)=ATMOSPHERIC PRESSURE
C     PROP2(5)=SCRATCH SPACE (NOT USED)
C     PROP2(6)=SCRATCH SPACE (NOT USED)
C     PROP2(7)=COEFFICIENT OF LATERAL EARTH PRESSURE, KO
C
C     STRESS(1-6) CONTAINS THE ELEMENT STRESSES.
C     STRESS(7) CONTAINS THE PORE PRESSURE.
C     STRESS(8-13) CONTAIN THE ELEMENT STRAINS.
C     STRESS(14) CONTAINS THE YIELD FUNCTION.
C
      IMPLICIT REAL*8(A-H,O-Z)
      DIMENSION STRESS(14),PROP1(7),PROP2(7)
      COMMON/EUBLK/ISTEP,NSTEP,KSTEP,IFGA
```

```
      DATA NENTER/0/
      IF(NENTER.NE.0) GO TO 6
      NENTER=1
C
      READ(5,4) NN,NEB
C
C     NN IS THE NUMBER OF FINITE ELEMENTS.
C     NEB IS THE DEBUG OUTPUT LEVEL.
C
    4 FORMAT(2I5)
    6 CONTINUE
      STRESS(14)=0.D0
C
C     CALCULATE THE PRINCIPAL STRESSES, S1 AND S3.
C
      STRES2=-(STRESS(2)+STRESS(7))
      STRES1=-(STRESS(1)+STRESS(7))
      CC=(STRES1+STRES2)/2.D0
      BB=(STRES1-STRES2)/2.D0
      CR=DSQRT(STRESS(4)*STRESS(4)+BB*BB)
      S1=CC+CR
      S3=CC-CR
C
C     UPDATE THE ELEMENT NUMBER, ISTEP.
C
      ISTEP=ISTEP+1
C
C     GET NEW TANGENT MODULUS AND POISSON'S RATIO.
C
   29 CALL EUD(ET,UT,STRESS,PROP1,PROP2,CR,S1,S3,ISTEP,NEB)
C
      IF(NEB.GT.1) WRITE(6,203) ISTEP
  203 FORMAT('ELEMENT',I5)
C
C     COMPUTE THE BULK MODULUS AND STORE IT IN THE
C     LOCATION OF POISSONS RATIO, UNLESS THE ELEMENT
```

```
C       HAS FAILED.
C
        IF(UT.EQ.0.0D0) GOTO 9100
        UT=ET/(3.D0*(1.D0-2.D0*UT))
 9100   CONTINUE
        IF(ISTEP.NE.NN) GO TO 40
        IF(NEB.GT.1) WRITE(6,24) NN
   24   FORMAT('THE NUMBER OF ELEMENTS IS=',I4)
   38   ISTEP=0
   40   CONTINUE
C
C       ET IS YOUNG'S MODULUS.
C       UT IS THE BULK MODULUS.
C
C
        CR=2.D0*CR
        IF(NEB.GT.1) WRITE(6,100) CR
  100   FORMAT ('S1-S3=',G15.5)
        IF(NEB.GT.1) WRITE(6,202) ET,UT
  202   FORMAT('MODULUS =',G15.5,10X,'BULK MODULUS=',G15.5 )
C
        RETURN
        END
END OF FILE
```